Aspects of a High Intensity Neutron Source

by

Peter H. Chapman

B.S., Engineering Physics (1998)
United States Military Academy

Submitted to the Department of Nuclear Science and Engineering
in partial fulfillment of the requirements for the degree of

Master of Science in Nuclear Science and Engineering

at the

MASSACHUSETTS INSTITUTE OF TECHNOLOGY

June 2010

Author . . . .
Department of Nuclear Science and Engineering
May 14, 2010

Certified by . . . .
Richard C. Lanza
Senior Research Scientist
Thesis Supervisor

Certified by . . . .
Gordon E. Kohse
Principal Research Engineer
Thesis Supervisor

Certified by . . . .
Jacquelyn C. Yanch
Professor of Nuclear Science and Engineering
Thesis Reader

Accepted by . . . .
Jacquelyn C. Yanch
Chair, Department Committee on Graduate Students

Aspects of a High Intensity Neutron Source

by

Peter H. Chapman

Submitted to the Department of Nuclear Science and Engineering
on May 14, 2010, in partial fulfillment of the
requirements for the degree of
Master of Science in Nuclear Science and Engineering

Abstract

A unique methodology for creating a neutron source model was developed for deuterons and protons incident on solid phase beryllium and lithium targets. This model was then validated against experimental results already available in literature. The model was found to adequately characterize the deuteron reactions, subject to the end user's desired tolerances, but only marginally so for the proton reactions.

A nonstandard, yet practical, application of such a neutron source model was demonstrated by conducting activation analysis for materials reasonably likely to be components in an accelerator based neutron source. This analysis consisted of inducing activation by exposure in the MITR-II 5 MW research reactor, and then adjusting the results based on the model's calculated neutron response. The analysis thus illustrated the utility of the source model in characterizing the system, enabling component design and evaluation before fabrication.

Thesis Supervisor: Richard C. Lanza
Title: Senior Research Scientist

Thesis Supervisor: Gordon E. Kohse
Title: Principal Research Engineer

Thesis Reader: Jacquelyn C. Yanch
Title: Professor of Nuclear Science and Engineering

Acknowledgments

I would like to thank a host of people that have helped me complete this thesis, understand the workings of a complex project and its associated schedule, cut and stack polyethylene shielding, count photons, run an MCNPX model, travel to and from Middleton, MA, etc. All of these people have helped me on a personal level in one regard or another. In alphabetical order, grouped by loose association, and by no means an exhaustive list, they are:

from the Bates Linear Accelerator Center: Peter Binns, Karen Dow, Gerry Fallon, Ken Hatch, Ernie Ihloff, Brian McAllister, Barbra McLaughlin, Hamid Moazeni, and Chris Tschalaer;

from L3: Sal Gargiulo, Ron McNabb, Dave Perticone, and Vitaliy Ziskin;

from the Laboratory for Nuclear Science: Jerry Fiumara, Ken Hewitt, and Jack McGlashing;

from MIT: Tom Bork, Jianmei Che, Gordon Kohse, Richard Lanza, Ed Lau, Tom Newton, and Jacquelyn Yanch;

and, from Home: my wife (easily the most important person mentioned), Tiffany.

I would like to specifically acknowledge Gordon Kohse, Richard Lanza, Dave Perticone, and Vitaliy Ziskin for their attention in devloping my scientific, system management, data analysis, and teaching abilities – as well as my New England cultural awareness.

Contents

List of Figures

List of Tables

Chapter 1

Introduction and Organization

Accelerator based neutron sources allow for a great deal of flexibility for industrial and research applications. Often, an intended application requires a certain neutron energy within a specific tolerance in order to induce a desired nuclear reaction. Based on these systems' complexity and cost, it is often desirable to create a working system model that reasonably predicts system performance and operating characteristics as a validation of key concepts prior to committing capital resources to their construction. This thesis explores one component of such a system; the model of a neutron spectrum created as a result of an accelerator based ion-target interaction at a specified incident ion energy.

The interaction between the accelerator's ions and target is the keystone of a complete system model. As the first component, the resulting spectra of the ion-target interaction is the source on which everything else, from the desired nuclear reactions to the ultimate deposition of energy in the system's detectors, depends. Thus, having a reasonably accurate source spectrum is a necessary part of a system model utilizing an accelerator based neutron source.

There are two avenues to producing a neutron source spectrum, discounting direct experimental evaluation of the proposed configuration: using tabulated experimental data, or using a computer based modeling approach. While the former may be available in some instances, the data may not exist for the desired spectra, or may be inconsistent across sources. Traditional nuclear codes, such as MCNP or GEANT,

are bound by similar limitations as they are based on existing libraries of data, and are therefore not suitable in the absence of evaluated data. Therefore, a need exists to utilize other simulations/models to create the required spectra when these libraries do not exist. Chapter 2, The Source Model, describes the creation of one such model by utilizing a combination of existing programs in a unique methodology. The model described in this chapter begins with accelerated ions incident on a solid phase target material and concludes with example outputs available from the source model.

This model is then validated in Chapter 3, Model vs. Experimental Data, through comparison of neutron spectra to experimental data for several ion-target combinations at different incident energies. These ion-target combinations consist of low atomic number, solid phase targets with prolific neutron production and relative ease of use, but whose responses are difficult to calculate. Additionally, evaluated data libraries do not exist or are sparse for these combinations; however, enough published data do exist with which to evaluate the model. The comparison data were not collected as part of this thesis, but were culled from available published sources describing deuterons and protons incident upon both beryllium and lithium. The predominant source of data is Guzek [4], but also includes deuterons incident on beryllium results from Whittlestone [12, 13] and Baumann [2, 3].

The most obvious use of the neutron source spectrum created by this model is to characterize the intended nuclear interactions of the system and follow the resultant signal to its conclusion, i.e., model the neutron induced reactions on which the system is to be based, and continue through to the response of the system's detectors. However, other less direct applications are also possible. Because neutrons exiting the target after their creation have the potential to interact with many materials before their intended application, their intermediate interactions are also of concern in a complete system model, notably with respect to activation. The target housing is arguably one of the more significant components in terms of neutron induced activation due to the proximity to the target, and thus the large flux experienced.

Chapter 4, Activation Analysis, examines this process by considering the induced activity expected from various materials likely to be utilized as a target holder. Al-

though the results are described as being related to target holders, they are not necessarily limited by the materials' applications. This chapter utilizes data obtained as part of this thesis from exposing a variety of materials to a neutron flux from the MITR-II 5 MW research reactor. The reactor induced activation was examined and analyzed in conjunction with the created source model to examine each material's activity characteristics. This comparison serves as an example of the type of analysis possible using the source model, and demonstrates its utility in system design where it is desirable to examine and/or adjust components prior to their manufacture.

The methodology developed in creating the source model is explained in greater detail with appropriate scripts and code in the appendices. Appendix A, TALYS Keyword Test, describes how the model was adjusted to match published experimental results to the extent possible. Appendix B, Multi-Energy TALYS Calculation, provides the script used in bridging the results from one of the model's components to the inputs in another used in calculating the neutron source spectrum. A simplifying assumption regarding the cross sections utilized in compiling the model's results is explained in Appendix C, Non-Elastic Calculation. Finally, the script used to collate and compile the calculations into useable results is presented in Appendix D, TALYS Processing with MATLAB.

Ultimately, modeling the results of the initial ion-target interaction facilitates understanding of the accelerator-target behavior and output characteristics, enables better downstream system modeling, and allows the adjustment of design parameters to ensure specific neutron source characteristics for an intended application. It is the goal of this thesis to present a method of modeling this interaction that can then be satisfactorily incorporated into a larger system model.

Chapter 2

The Source Model

2.1 Model Overview

This chapter considers an accelerator producing deuterons at 4 MeV and a thick, solid beryllium target as the vehicle with which to explore the means to create an ion-target source model. This configuration was chosen based on the range of available experimental data with which to compare the model, as well as the availability of commercially produced deuteron accelerators and the prolific nature of the $^9\text{Be}(\text{d,n})^{10}\text{B}$ reaction. Additionally, beryllium has the desirable characteristics of high melting point and stability, as compared to other solid targets such as lithium (which will also be examined in Chapter 3)[4].

The approach used to create the source spectra is to combine several programs' calculations into one model. First, the potential deuteron reaction energies are calculated after accounting for the ions slowing down within the target material. The relevant cross sections are then calculated for each energy, along with the associated output particle spectra. Finally, the results for each energy are merged to provide neutron output spectra for the specific ion energy-ion-target configuration.

The primary tools used in this methodology are SRIM/TRIM and TALYS, with a UNIX shell script and a MATLAB script used to unify and synthesize these programs' results. SRIM/TRIM is a Monte Carlo program that uses a quantum mechanical treatment of ion-atom collisions to calculate the stopping and range of ions in

matter [14, 15]. A UNIX shell script was used as a bridge between the output from SRIM/TRIM calculations and the input required for TALYS.

TALYS is a nuclear reaction program that calculates a complete chain of nuclear reactions using a variety of models. These models include optical, fission, and direct, compound, and pre-equilibrium reactions.[1] The calculation begins with a specified incident particle and energy as it interacts with the target nucleus and induces various nuclear reactions. Each possible competing reaction channel is examined, and the characteristics of the residual nucleus and ejected particles are calculated. TALYS loops over all such possibilities recursively until all reaction channels are closed [7, 8]. The TALYS outputs were synthesized into emission spectra by using a MATLAB script.

2.2   Implementation using ^{9}Be(d,n)^{10}B at 4 MeV

SRIM was utilized to first determine the range of deuterons in a solid beryllium target by simulating 2,500 4 MeV heavy hydrogen ions impinging on a pure beryllium mass.[2] This result was considered the minimum thickness of the target to be considered experimentally thick, preventing ion transmission through the target, and was rounded arbitrarily higher for the remainder of the calculations in order to ensure all incident deuterons stopped inside the target.

With the thickness of the target determined, TRIM was utilized to determine the Bragg curve of the ions, and the energy lost at a particular depth inside the target. This process created equal depth bins within the target, each with a corresponding reaction energy. These energies were then utilized as inputs in the TALYS calculations to account for the slowing down of the ions within the target material.

TALYS requires only four parameters to describe an interaction; however, there are numerous other parameters the user can adjust in order to fine tune the calculation's

---

[1]The TALYS distribution includes a users manual that provides a full description of the models utilized and their method of calculation. It also includes the source code for all subroutines, including a modified version of the ECIS-06 reaction code.

[2]SRIM/TRIM do not allow the explicit entry of deuterons; however, it allows adjusting the mass of elemental ions. Deuterons were thus created by adjusting the hydrogen ion's mass to 2.0136 amu.

results.[3] This thesis utilized a brute force method of determining which of the optional keywords were beneficial, and attempted to optimize their values in order to more closely approximate published data. In the case of the ^{9}Be(d,n)^{10}B reaction at 4 MeV, the test was run by initially considering a single incident energy, looping over selected keywords and values, and then comparing the results to published data for the 0 degree output neutron spectrum. The script for this process can be found in Appendix A.

With the needed modifier keywords determined, TALYS was run once for each energy, as determined by the TRIM simulation, in order to account for the ions' loss of energy within the target.[4] The UNIX script controlling this process can be found in Appendix B. The input files also included flags, as shown in Table 2.1, to produce the *XspecYYY.YYY.lab* and *XddxZZZ.Z.lab* files. These files record the calculated differential cross section $[mb/MeV]$ and double differential cross section $[mb/MeV/sr]$, respectively, for particle X of incident energy $YYY.Y$ and output angle $ZZZ.Z$ in the lab frame of reference.

Each output file also recorded the calculated non-elastic and particle production cross sections, which could then be utilized to compute particle production weights that considered elastically scattered incident particles to still be available for a non-elastic event. This method, described in Appendix C, resulted in less than a one percent improvement over using the total production cross sections, and in the interest of simplicity, was not used.

The TALYS *.spec* and *.ddx* files were then processed in MATLAB utilizing the script provided in Appendix D. The angle integrated *.spec* files were processed by reading them into a data array, adjusting to a common outgoing neutron energy index, and then computing the yield from the interpolated differential cross sections. The angular spectra from the *.ddx* files were processed in a similar fashion.

---

[3]The required parameters are the projectile, projectile's energy, target element, and target mass. Over 230 additional keywords are available to control nuclear model parameters, output values calculated, and output information files and formats.

[4]TALYS allows for the inclusion of a range of energies as an input parameter, thereby enabling a multiple energy calculation from one input file. However, this thesis created a separate input file for each energy in order to facilitate reading the data into multidimensional arrays within MATLAB.

Table 2.1: Base keywords used in TALYS calculations

Keyword	Value	Description
recoil	y	Flag for the calculation for the recoils of the residual nuclides and the associated corrections to the light particle spectra
labddx	y	Flag for the calculation of double differential cross sections in the lab system (requires *recoil y*)
outangle	y	Flag for the output of angular distributions for scattering to discrete states
outspectra	y	Flag for the output of angle integrated emission spectra
ddxmode	2	Option for the output of double differential cross sections, providing the output per emission angle as a function of energy
filespectrum	n	Designator for the output of the composite particle spectrum for neutrons in a separate file (requires *outspectra y*)
fileddxa	various	Designator for the output of double differential cross sections per emission angle for the particle specified (in this case, neutrons).

2.3 Results

The result of these calculations is the creation of matrices that record the neutron emission spectra as a function of input energy and output angle; examples from calculating the ^{9}Be(d,n)^{10}B reaction with an incident deuteron energy E_d of 4 MeV are graphically depicted in Figures 2-1 through 2-4.

Figures 2-1 and 2-2 show angular spectra created by the source model after processing of the *.ddx* files. These curves are integrated over all contributing incident deuteron energies. Figure 2-1 shows the normalized TALYS calculated 0 degree emission spectrum (in the lab frame of reference and after keyword optimization) for the ^{9}Be(d,n)^{10}B reaction with E_d of 4 MeV as compared to published experimental data from Guzek [4]. The 0 degree spectrum is the one used to adjust the source model to experimental results to the extent possible through the keyword optimization process. Figure 2-2 displays the neutron angular spectra produced by the reaction, with angles measured in the lab frame of reference. Analyzing the angular spectra allows the addition of the outgoing neutron angle as a system design parameter, enabling

the user to potentially refine the desired neutron response by selectively choosing the output angle.

Figures 2-3 and 2-4 show energy spectra created by the source model after processing the *.spec* files. These curves are integrated over all outgoing neutron angles. Figure 2-3 displays the spectra created by different incident energies, each corresponding to the depth bins from the SRIM/TRIM simulation. These spectra show how a single energy inadequately describes the complete neutron response, thereby illustrating the necessity of accounting for the ion's loss of energy as it travels through the target material. Finally, Figure 2-4 shows the result of combining all possible incident energies and outgoing angles, and displays the total neutron yield curve from the deuteron on beryllium reaction, measured over 4π.

It is important to note that this application of TALYS is not included as an intended use by its authors due to the low mass number of the target. The specified mass number range for TALYS is 12-339, where the nuclear models implemented within the code have been validated in the literature. The TALYS user manual explores a variety of test cases within this range and compares them to experimental results, in order to give the user a sense of the program's capabilities and limitations. In a sense, this thesis is an extension of those comparisons, with some modifications and the recognition that the code is being used outside it's recommended parameter range. Despite falling outside the TALYS authors' intended applications, the source model created in this thesis produces results that may be used to address a need when creating an accelerator based neutron source as part of a larger system. The following chapter examines these results via comparison to available experimental data for a variety of ion-target combinations.
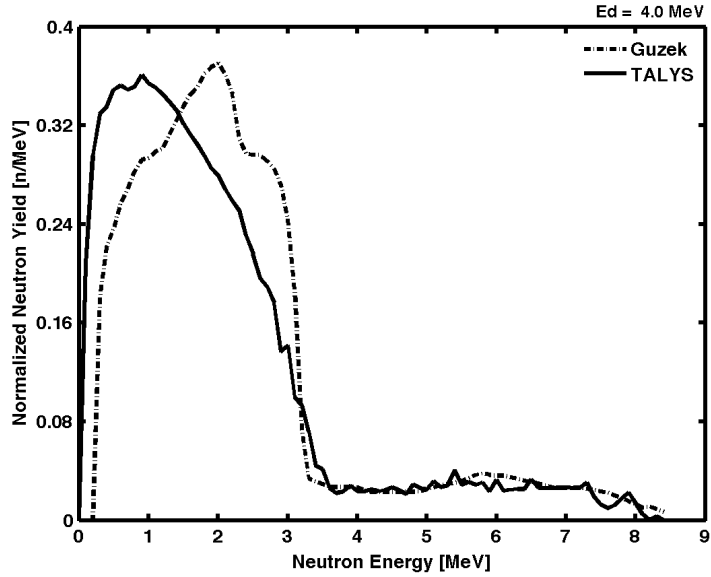
Figure 2-1: TALYS calculated (solid line) and Guzek results (dashed line) normalized neutron spectrum for the ^{9}Be(d,n)^{10}B reaction with E_d of 4 MeV at 0 degrees. The 0 degree curve was used during keyword identification and optimization during comparison to published experimental results; the TALYS curve presented reflects the optimized spectrum as a result of this process.
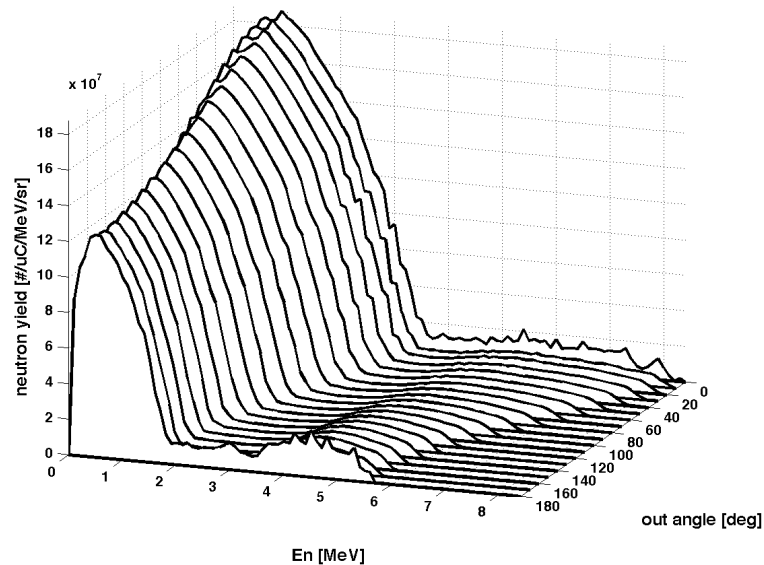

Figure 2-2: TALYS calculated neutron spectra E_n for the ^{9}Be(d,n)^{10}B reaction with E_d of 4 MeV as a function of outgoing neutron angle in the lab frame of reference. This plot illustrates the model's ability to incorporate the outgoing neutron angle as a system design parameter.
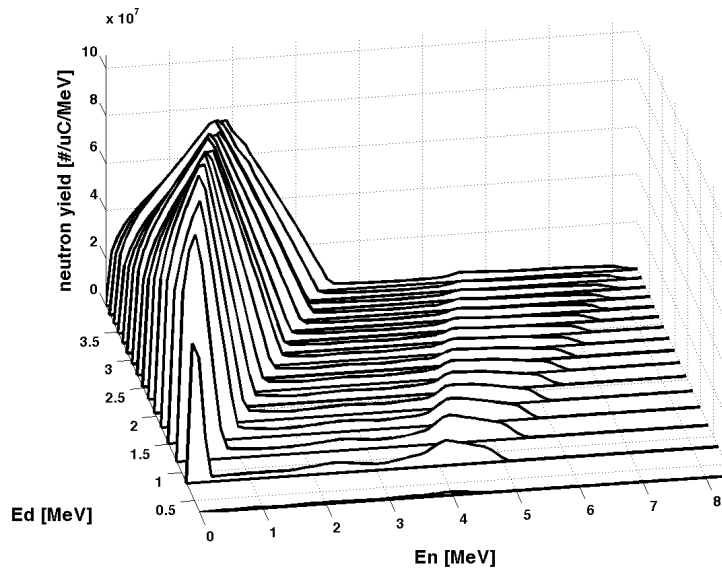
Figure 2-3: TALYS calculated neutron spectra for the ^{9}Be(d,n)^{10}B reaction with E_d of 4 MeV as a function of incident deuteron energy determined by TRIM. This plot illustrates the necessity of accounting for the incident ions slowing down within the target material and undergoing reactions at different energies.
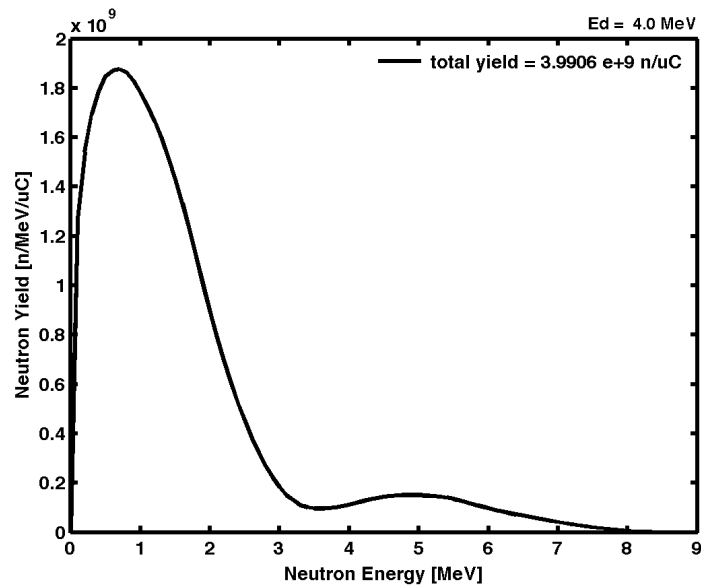

Figure 2-4: TALYS calculated angle integrated spectrum for the ^{9}Be(d,n)^{10}B reaction with E_d of 4 MeV. This plot represents the complete neutron spectrum produced over 4π at the point of ion-target interaction.

23

Chapter 3

Model vs. Experimental Data

3.1 Comparison Overview

This chapter presents the results of the SRIM/TALYS generated source model for both protons and deuterons incident on both lithium and beryllium, and compares these results to experimental data. The primary experimental data set utilized for these comparisons is the Guzek thesis [4], due to the variety and compactness of data contained therein. Other data sets utilized for the comparison of the d,Be reaction include Whittlestone [12, 13] and Baumann [2, 3].[1] A summary of the comparisons made can be found in Table 3.1.

The published data were processed via Engauge Digitizer, an open source software package that facilitates the conversion of an image file into data arrays, on a Windows XP SP3 machine [9]. The digitization process facilitated the comparison of experimental data with the TALYS calculated results.

The 2008 version of SRIM/TRIM was utilized during this thesis, and calculations were conducted on a Windows XP SP3 machine. TALYS calculations were conducted on a Fedora 10 machine using TALYS version 1.5, a pre-release of version 1.2, after compiling the code with PGF90 6.0-4, a 32 bit x86 Linux Portland Group FORTRAN compiler.[2]

---

[1]The experimental data used in this thesis were not collected as part of the thesis, but were obtained from previously published results.

[2]Compiler selection is important and affects results. The PGI compiler was utilized after discov-

Table 3.1: Summary of TALYS-experiment comparison combinations.

Inc. Particle	Target	Energy [MeV]	Exp. Data	Figure	Page
d	Be	0.90	Guzek	3-2	31
		1.50			
		4.00		3-3	32
		2.80	Whittlestone	3-4	33
		7.50	Baumann		
	Li	0.90		3-6	37
		1.50			
		4.00		3-7	38
p	Be	2.57	Guzek	3-8	41
		3.00			
		4.00		3-9	42
	Li	2.32		3-10	44
		4.28			

The TALYS results were adjusted for each ion energy-ion-target combination to the extent possible in order to match the experimental data offered at a 0 degree output angle, with the goal of producing a set of keywords and values that were consistent across the incident energies examined. The hope of this approach is that the optimized set of keywords can then be utilized for other incident energies with the same ion-target combination while giving the user some idea as to the degree of confidence the results warrant. For those combinations whose reactions required keyword adjustments, a graph is presented showing the effects of each keyword in isolation and in total at a representative incident energy for the 0 degree response curve.

The comparison of results for each ion energy-ion-target combination is presented as a series of three graphs, the first of which is the normalized 0 degree yield curve used in keyword identification and optimization. The purpose of this plot is to give the user a sense of the accuracy of the TALYS calculations with respect to the reaction's neutron response. Additionally, this curve represents the probability density function that could be utilized as the neutron source in a subsequent model utilizing a Monte Carlo engine. In each of these plots, the TALYS calculated results are presented as a

ering that GNU FORTRAN compilers produced nonsensical results.

solid line, while the experimental data are presented with a dashed line.

The second plot shows neutron yield as a function of outgoing angle in units of n/sr/μC for TALYS and experimental data. The raw TALYS results, in units of n/sr/incident particle, were adjusted to match the units of the experimental results by multiplying by a conversion factor of 6.24 x10^{12} incident particles/μC. Again, the solid line represents the TALYS results, while the dashed line represents experiment. However, in order to quantify the difference between the two sets of data, a third, light dashed line has been added to annotate their difference. This difference d is calculated by

$$d = \left| \frac{T - E}{E} \right| * 100\% \ , \tag{3.1}$$

where T and E represent the yield for TALYS and experimental results respectively. These data were not available for the Baumann results; however, the TALYS results are presented for completeness.

Finally, the third plot shows the TALYS calculated neutron response over all angles. This plot is essentially the superposition of all contributions arising from each SRIM/TRIM calculated incident energy, such as presented in Figure 2-3. Data were available for a direct comparison in the case of Whittlestone's results, and these have been included in Figure 3-4c. The integral of the TALYS calculated total neutron response is also presented within the plot as the total neutron yield per μC.

These three plots facilitate a comparison in terms of response behavior and angular yield. For comparison purposes in this thesis, the response behavior is further subdivided into peak energy location, locations of sharp increases/decreases, relative heights of broad energy groups, and relative smoothness of response. Although the intended application of the source model will dictate what is ultimately acceptable to the user, this thesis considers agreement along most of the comparative points, as well as having some degree of adjustability available, to constitute a suitable model.

3.2 Deuterons incident on Beryllium

The keywords utilized in the TALYS calculations are listed in Table 3.2, and their effects are illustrated for an incident deuteron energy of 4.0 MeV in Figure 3-1. Figure 3-1 is presented as the neutron yield curve prior to normalization in order to facilitate a comparison in terms of response and 0 degree yield.

Table 3.2: ^{9}Be(d,n)^{10}B TALYS keywords

| Keyword	Value	Description
angles	10	Number of emission angles for reactions to discrete states
gammashell1	0.70	Constant for the global expression for the damping parameter for shell effects in the level density parameter γ
maxlevelsbin	n 4	The number of included discrete levels for the neutron channel resulting from binary emission that is considered in Hauser-Feshbach decay and the gamma-ray cascade

In general, the TALYS calculated neutron response approximated the experimental results across the range of incident energies examined.

For incident energies below 2 MeV, the model's response included most of the intermediate energy peaks between 1 and 5 MeV. At incident energies above 2 MeV, the TALYS results mirrored the approximate locations of the broad energy peaks. However, the peak energy locations were different in all comparisons.

The model showed the significant rise in the lower energy response, although not as dramatically as shown through experiment. In particular, the middle three incident energies showed a gradual rise in yield at lower energies, whereas the experiments show a response approaching that of a step function.

TALYS shows a sizable response in the low energy spectrum for E_d of 0.9 MeV as a result of inclusion of the *gammashell1* parameter; however, this parameter was necessary to boost the low energy response at higher incident energies. The ratio of low to high energy neutron response does increase, as indicated by Guzek, for E_d over 1 MeV, although not quite as dramatically.

All plots were relatively smooth throughout their response. The higher incident

28
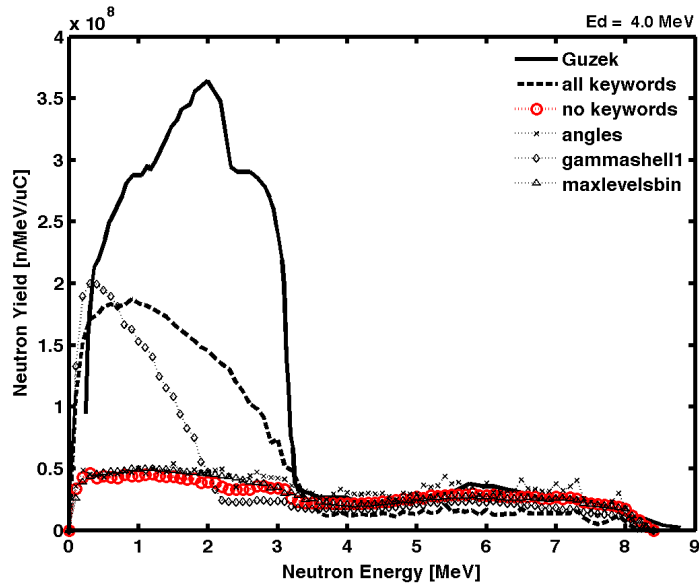
(a)
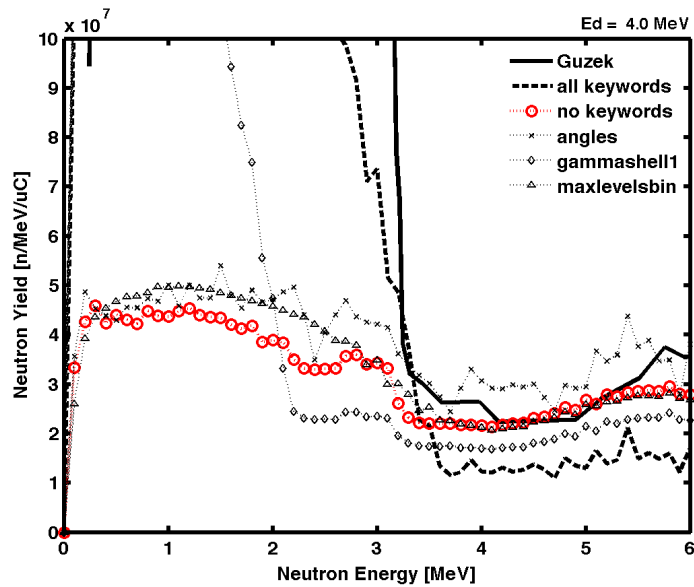
(b)

Figure 3-1: Keyword comparison for ^{9}Be(d,n)^{10}B at 4.0 MeV at full scale in subplot (a) and closer for clarity in subplot (b) prior to normalization. The solid line denotes the Guzek results, and the dashed line indicates TALYS calculation with the inclusion of all three indicated keywords. The circle markers indicate the TALYS calculations without any keywords, the cross markers illustrate the neutron response with the *angles* keyword, the diamond markers denote the *gammashell1* keyword, and the triangle markers show the effect of the *maxlevelsbin* keyword.

energies show some signs of erratic response behavior as a result of the *angles* keyword. This keyword was necessary in the formation of the intermediate energy peaks at the lower incident energies.

The angular yield response was within one order of magnitude for each energy; however, the TALYS results were monotonically decreasing at the lower energies, whereas the Guzek results indicated an increase in yield after 80 degrees. At energies above 2.8 MeV, the TALYS results were noticeably not as forward peaked as the experimental data. The ratio of angular yields is not consistent across the variety of energies, precluding the adjustment of the model by a multiplicative factor.
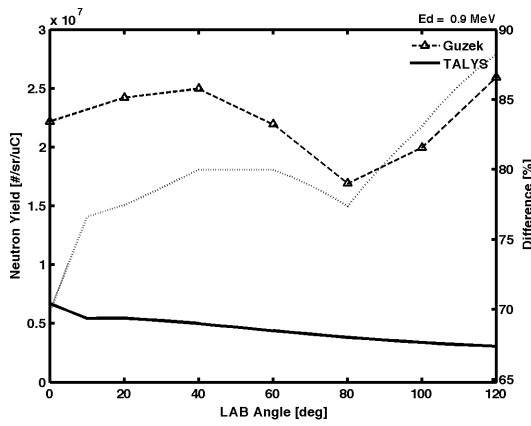
The significant drop in the low energy, around 1 MeV and below, response for the experimental results (notably the Baumann results) is due to the low energy cutoff of the electronics used in the experiments, and does not reflect the actual neutron response.
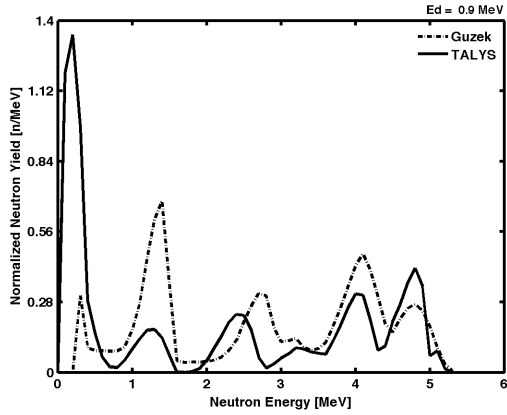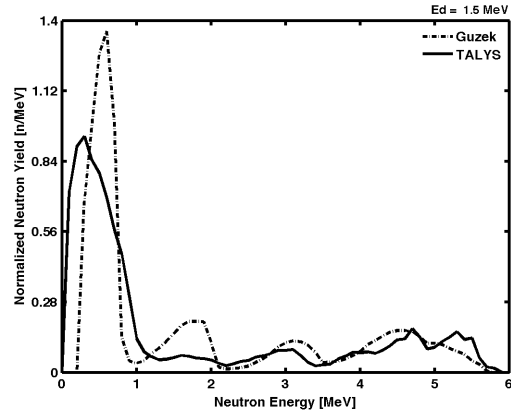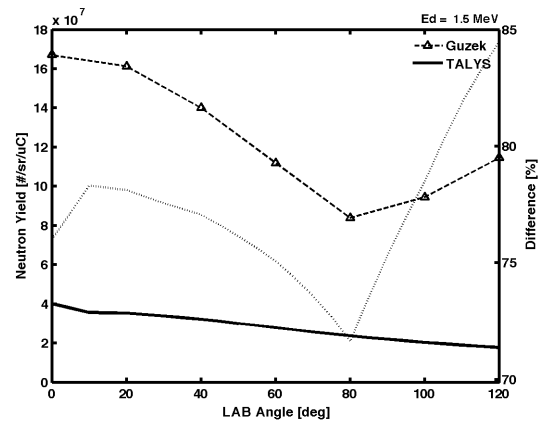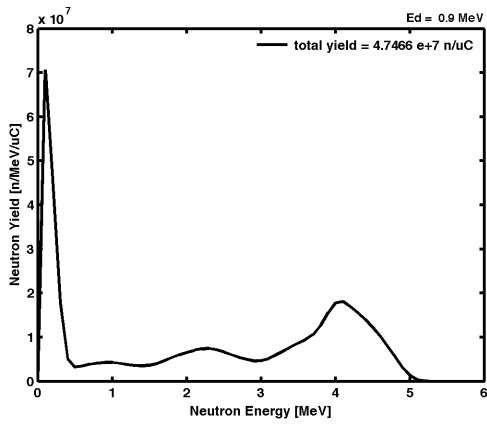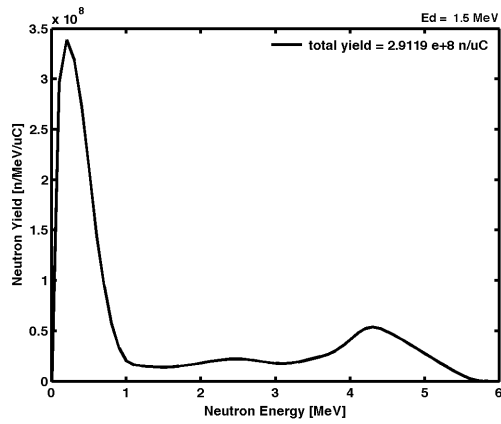
Figure 3-2: TALYS results for the ^{9}Be(d,n)^{10}B reaction for 0.9 MeV ((a)-(c)) and 1.5 MeV ((d)-(f)), as compared to Guzek's results. Plots (a) and (d) show the normalized 0 degree calculation used in TALYS keyword optimization, plots (b) and (e) show the TALYS calculated angular yields and their difference with Guzek's results, and plots (c) and (f) show the TALYS calculated angle integrated total neutron yield curves.
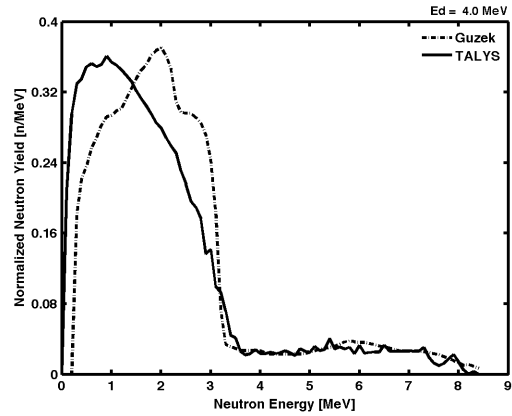
(a)
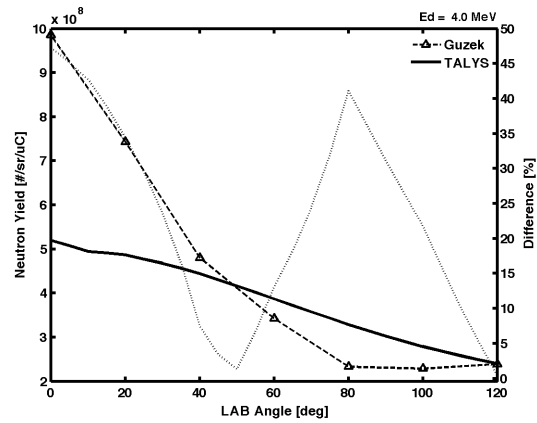
(b)
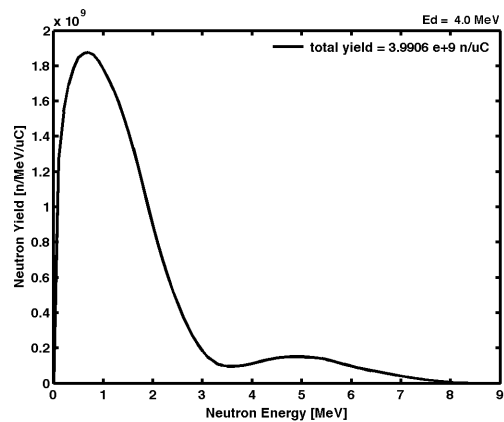
(c)

Figure 3-3: TALYS results for the ^{9}Be(d,n)^{10}B reaction for 4.0 MeV, as compared to Guzek's results. Plot (a) shows the normalized 0 degree calculation used in TALYS keyword optimization, plot (b) shows the TALYS calculated angular yields and their difference with Guzek's results, and plot (c) shows the TALYS calculated angle integrated total neutron yield curves.
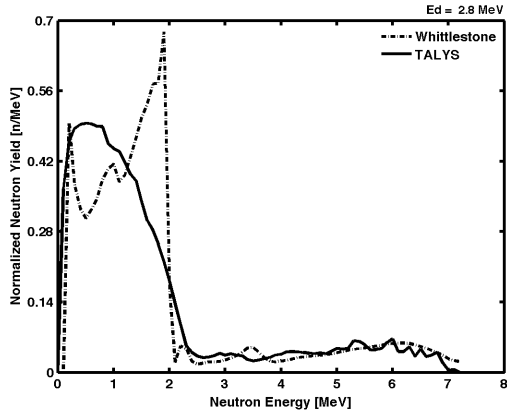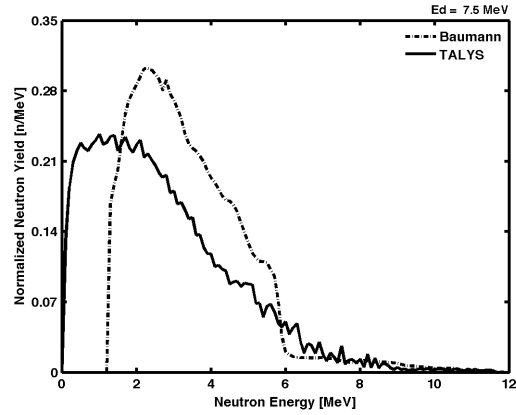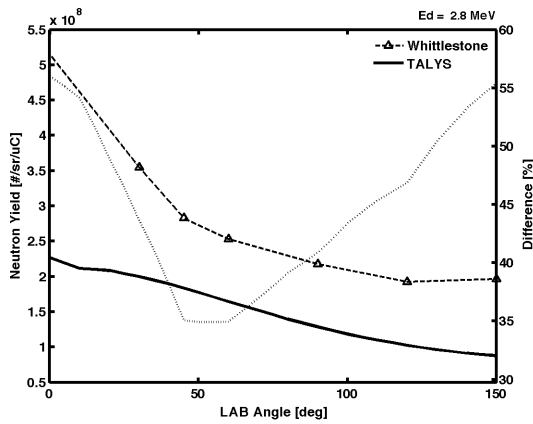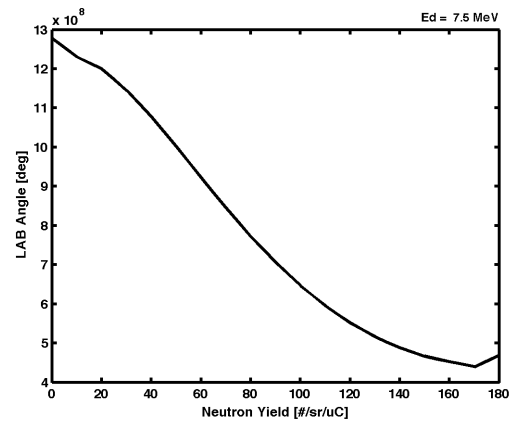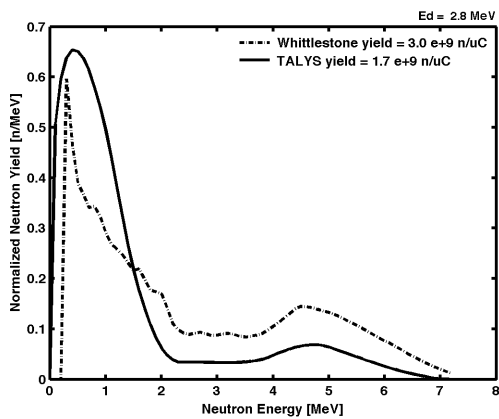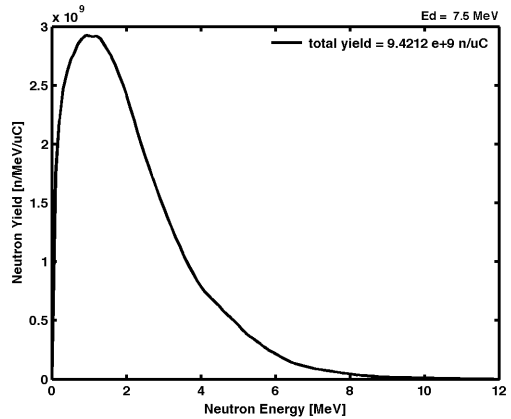
Figure 3-4: TALYS results for the ^{9}Be(d,n)^{10}B reaction for 2.8 MeV ((a)-(c), compared to Whittlestone's results) and 7.5 MeV ((d)-(f) compared to Baumann's results). Plots (a) and (d) show the normalized 0 degree calculation used in TALYS keyword optimization, plots (b) and (e) show the TALYS calculated angular yields, and plots (c) and (f) show the TALYS calculated angle integrated total neutron yield curves.

3.3 Deuterons incident on Lithium

The keywords utilized in the TALYS calculations are listed in Table 3.3, and their effects are illustrated for an incident deuteron energy of 4.0 MeV in Figure 3-5. Figure 3-5 is presented as the neutron yield curve prior to normalization in order to facilitate a comparison in terms of response and 0 degree yield. An important note for these keywords is that their effect on the neutron response is different when included separately than when included together. Figure 3.3 shows no difference between the unmodified TALYS calculation and when the *gammashell1* keyword is included by itself. However, when paired with the *maxlevelsbin* keyword, the effect is to increase the low energy response in a dramatically different way than with *maxlevelsbin* alone. Above approximately 2 MeV, the TALYS calculations are equivalent, regardless of keyword.

Table 3.3: ^{7}Li(d,n)^{8}Be TALYS keywords

Keyword	Value	Description
gammashell1	0.70	Constant for the global expression for the damping parameter for shell effects in the level density parameter γ
maxlevelsbin	n 4	The number of included discrete levels for the neutron channel resulting from binary emission that is considered in Hauser-Feshbach decay and the gamma-ray cascade.

In general, the TALYS calculated neutron response approximated the experimental results across the range of incident energies examined.

TALYS showed broad responses around 3 MeV and 12 MeV for the two low energy calculations, and a distinguishable low energy peak for the high energy calculation. These features mirror the gross neutron group characteristics identified and shown in Guzek. However, the peak energy locations were again different in all comparisons, although not quite as dramatically.

The model's response for the two lower incident energies showed the general features of the multiple energy groups, albeit in a more aggressive manner than indicated by Guzek. The 4.0 MeV response shows the appreciable increase in the low energy

(a)

(b)
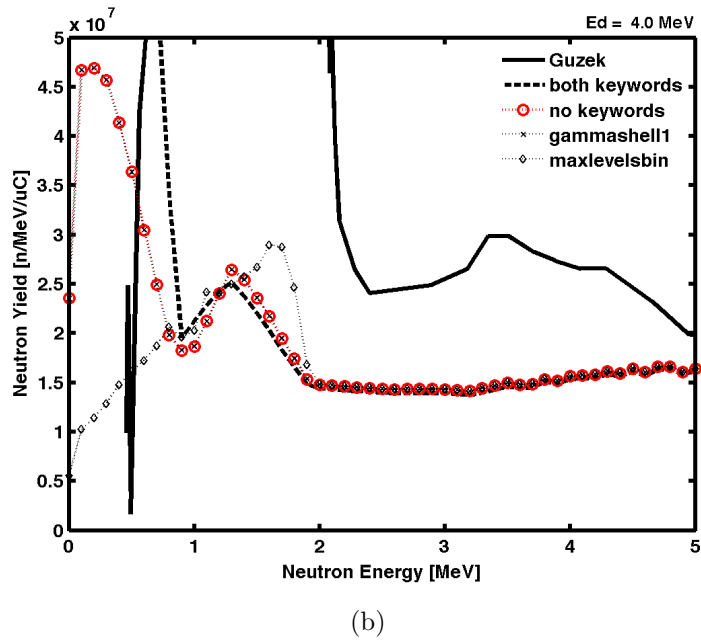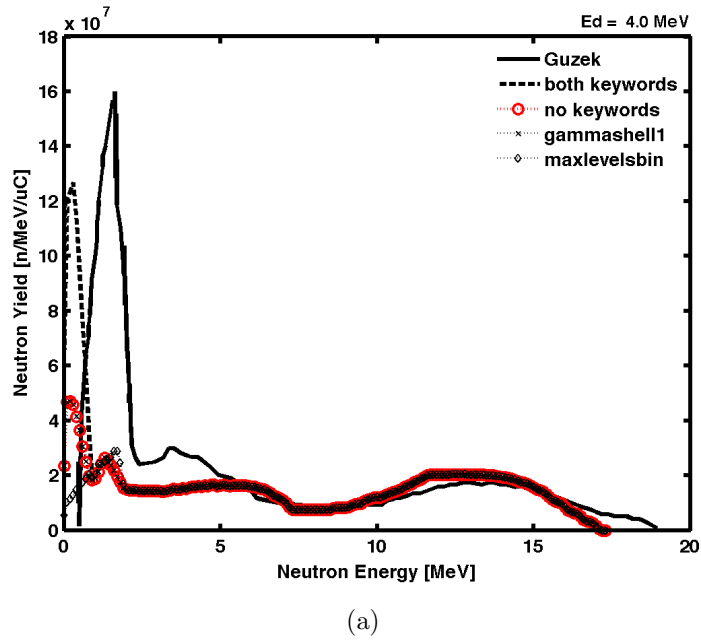
Figure 3-5: Keyword comparison for ^{7}Li(d,n)^{8}Be at 4.0 MeV at full scale in subplot (a) and closer for clarity in subplot (b) prior to normalization. The solid line denotes the Guzek results, and the dashed line indicates TALYS calculation with the inclusion of both indicated keywords. The circle markers indicate the TALYS calculations without any keywords, the cross markers illustrate the neutron response with the *gammashell1* keyword, and the diamond markers show the effect of the *maxlevelsbin* keyword.

response that occurs as higher energy states for the recoil nucleus become available at a slightly lower energy than experiment.

At an E_d of 0.9 MeV, the model indicates the ratio of low to high energy neutrons was greater than one, as shown by Guzek, but is not as successful for E_d of 1.5 MeV. The relative heights of the neutron groups at the highest incident energy nearly matches Guzek.

All plots were relatively smooth in their response, and the absence of the *angles* keyword precluded the introduction of erratic behavior at higher neutron energies.

The angular yield response was generally consistent, with the TALYS calculations falling within one order of magnitude from Guzek. The TALYS response was closest at higher energy; however that is not necessarily indicative of a trend as the intermediate energy showed the highest difference. For the two lowest incident energies, the angular yield at 0 degrees appears to be different by a factor of around 2, but this feature disappears at the higher E_d of 4 MeV and thus prevents modification of an adjusting function.
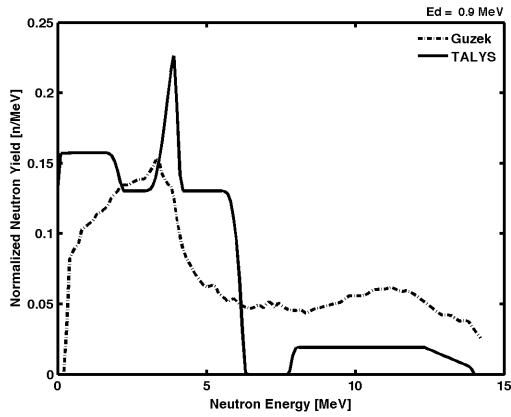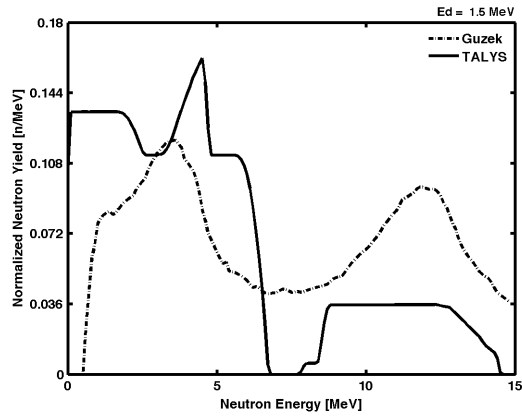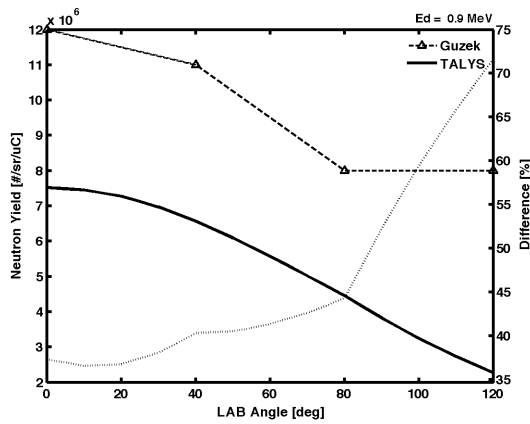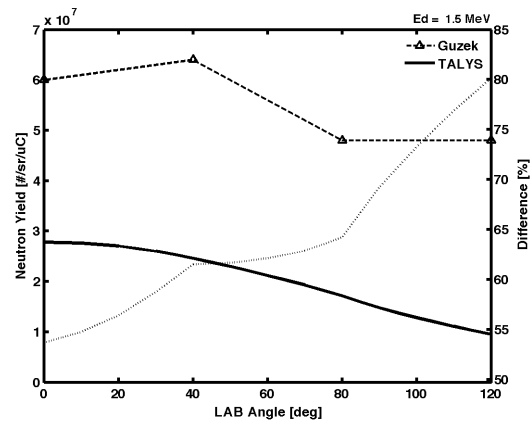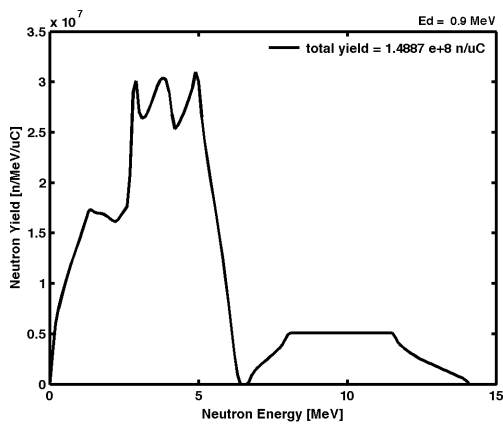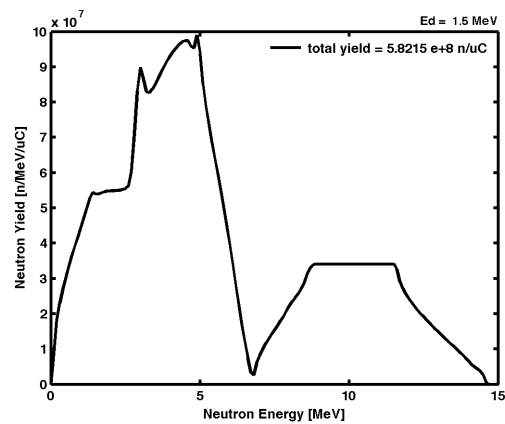
Figure 3-6: TALYS results for the ^{7}Li(d,n)^{8}Be reaction at 0.9 MeV ((a)-(c)) and 1.5 MeV ((d)-(f)), as compared to Guzek's results. Plots (a) and (d) show the normalized 0 degree calculation used in TALYS keyword optimization, plots (b) and (e) show the TALYS calculated angular yields and their difference with Guzek's results, and plots (c) and (f) show the TALYS calculated angle integrated total neutron yield curves.
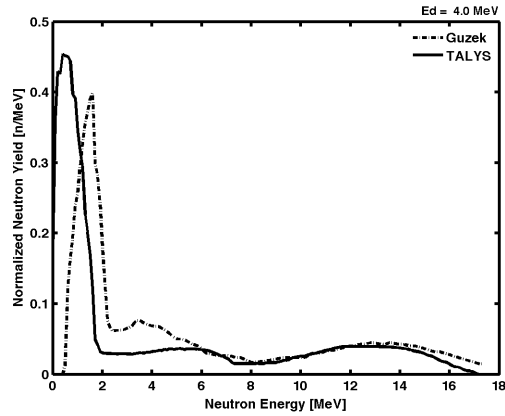
(a)
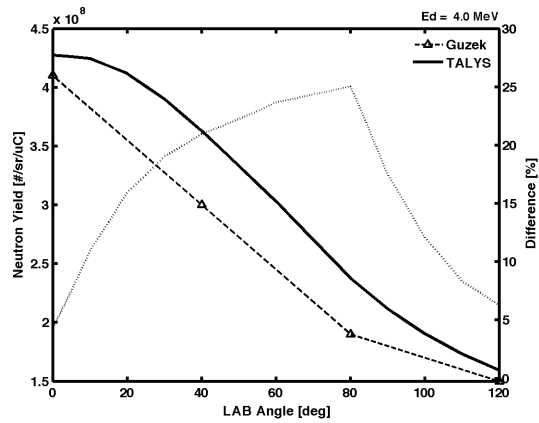
(b)

(c)

Figure 3-7: TALYS results for the ^{7}Li(d,n)^{8}Be reaction at 4.0 MeV, as compared to Guzek's results. Plot (a) shows the normalized 0 degree calculation used in TALYS keyword optimization, plot (b) shows the TALYS calculated angular yields and their difference with Guzek's results, and plot (c) shows the TALYS calculated angle integrated total neutron yield curves.

3.4   Protons incident on Beryllium

No keywords were identified that improved the match between calculated results and experimental data with any degree of significance. However, some improvement was seen when including all relevant energies offered by the TRIM calculation as inputs in the TALYS calculations. That is to say that because ^{9}Be(p,n)^{9}B has a Q-value of -1.85 MeV, corresponding to a threshold of about 2 MeV, it is not necessary to include reaction energies below 2 MeV. This reduction of energies has the effect of reducing the number of TALYS calculations that contribute to the overall result when maintaining the three energy interval used as the default in the model, and it was found that including all available energies offered by the TRIM calculation above the threshold energy smoothed the neutron response.[3]

In general, the TALYS calculated neutron response did not successfully approximate the experimental results across the range of incident energies examined.

The TALYS calculations did not reproduce the 0.6 MeV peak present in any of the three incident energies' response, and this feature is one of the more salient properties of the experimental results.

At the two lower incident energies, the nearly featureless response curves shown by experiment prevent a comparison regarding sharp increases/decreases and relative heights of neutron groups with the model's results. At a E_p of 4.0 MeV Guzek shows the beginnings of a secondary energy group around 2 MeV, and this is not seen in the model's results.

The two higher incident energies show erratic behavior throughout their response curve. The outgoing neutron energy mesh of 0.1 MeV, a fixed parameter of the TALYS calculation, appears to be too coarse.

The angular yield response was generally consistent, with the TALYS calculations being within one order of magnitude of Guzek. However, the TALYS results did not show the slight increase in yield past 80 degrees for the 4.0 MeV incident protons,

---

[3]This is in comparison to other reactions without a threshold, such as ^{9}Be(d,n)^{10}B, where a smooth response was obtained using only every third energy bin offered by the TRIM calculation. The default setting of selecting every third energy bin in the model was originally chosen in an effort to reduce computation time.

instead being monotonically decreasing for all examined energies. Again, two of the three examined incident energies showed what appears to be the potential for a corrective factor to the angular yield, but the relationship is not consistent and therefore not useful.
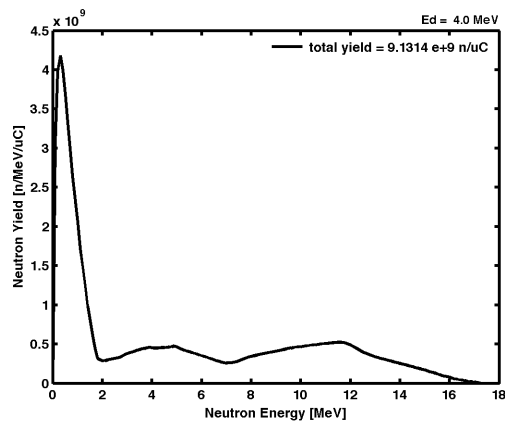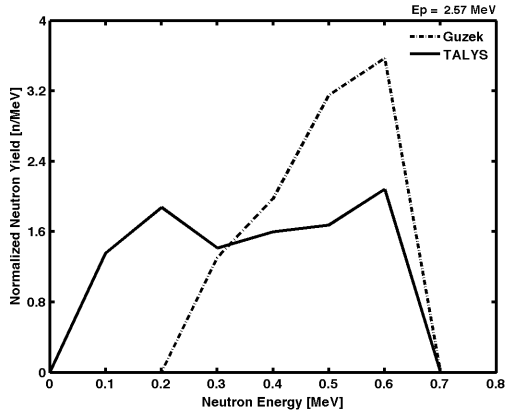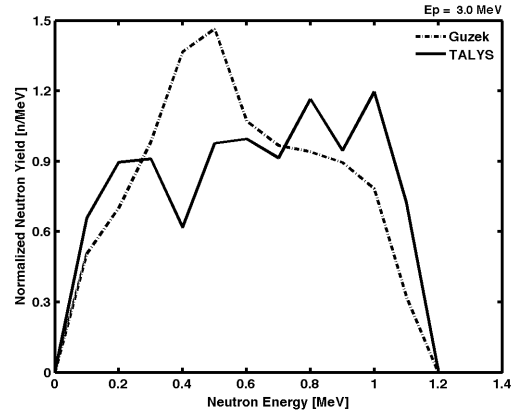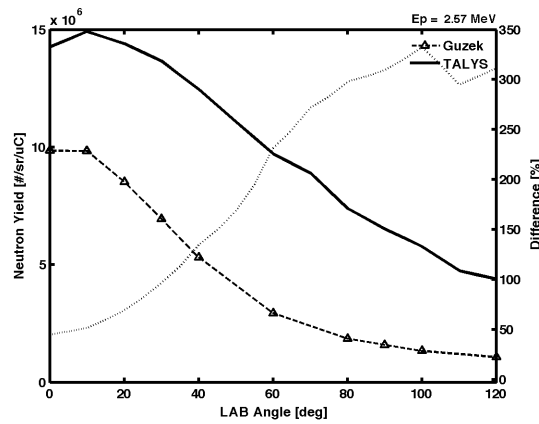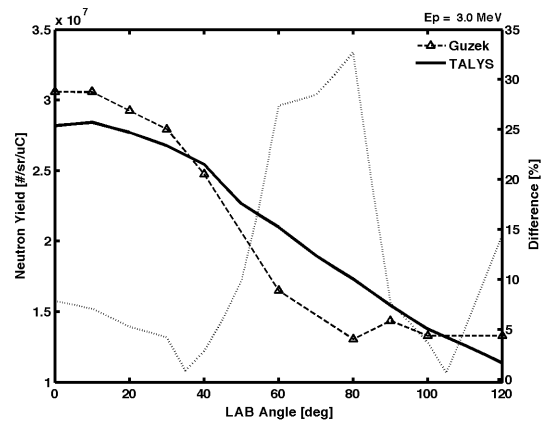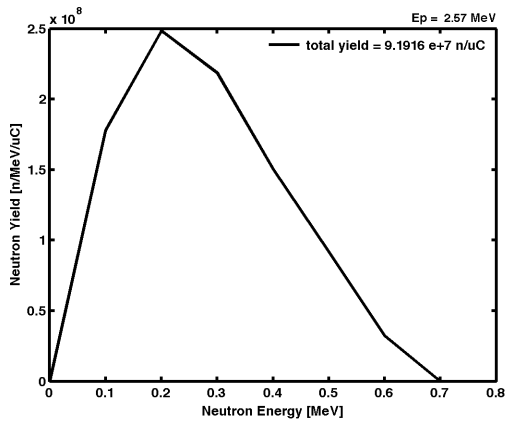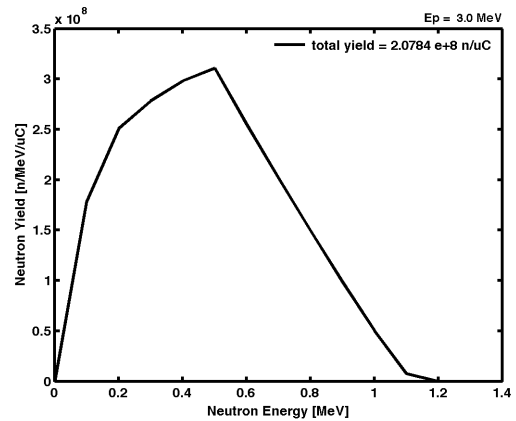
Figure 3-8: TALYS results for the ^{9}Be(p,n)^{9}B reaction at 2.57 MeV ((a)-(c)) and 3.0 MeV ((d)-(f)), as compared to Guzek's results. Plots (a) and (d) show the normalized 0 degree calculation used in TALYS keyword optimization, plots (b) and (e) show the TALYS calculated angular yields and their difference with Guzek's results, and plots (c) and (f) show the TALYS calculated angle integrated total neutron yield curves.

41
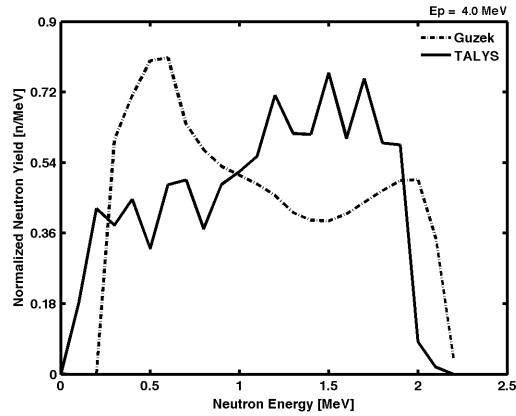
(a)
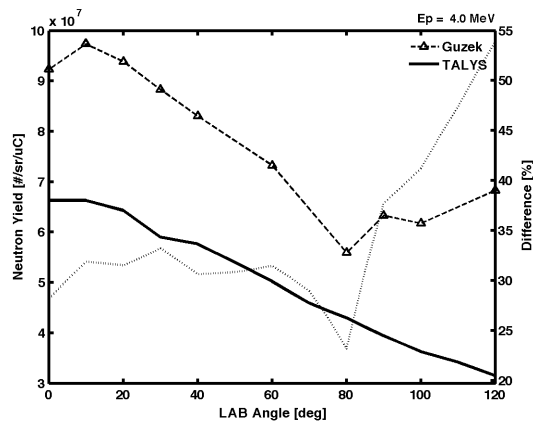
(b)
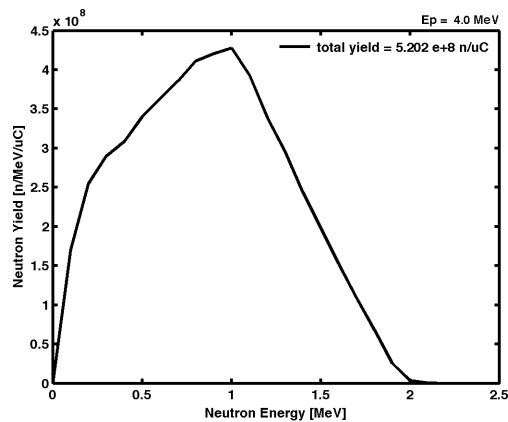
(c)

Figure 3-9: TALYS results for the ^{9}Be(p,n)^{9}B reaction at 4.0 MeV, as compared to Guzek's results. Plot (a) shows the normalized 0 degree calculation used in TALYS keyword optimization, plot (b) shows the TALYS calculated angular yields and their difference with Guzek's results, and plot (c) shows the TALYS calculated angle integrated total neutron yield curves.

3.5   Protons incident on Lithium

No keywords were identified that improved the match between calculated results and experimental data with any degree of significance. However, improvements were seen, as in the ^{9}Be(p,n)^{9}B reaction, by including all available incident energies resulting from the TRIM calculations.

In general, the TALYS calculated neutron response did not successfully approximate the experimental results across the range of incident energies examined.

The TALYS calculations did not reproduce the identifiable peak from Guzek for E_p of 2.32 MeV. The lack of a significant peak in the higher incident energy comparison prevents a worthwhile comparison for this factor.

For the lower incident energy, the model did not identify the two neutron groups seen in Guzek. The higher incident energy did not have separate neutron groups with which to compare the model.

At E_p of 2.32 MeV the model's response was too smooth, while at E_p of 4.28 MeV the model showed erratic behavior and showed features not present in the experimental response.

The angular yield response was generally consistent, with the TALYS calculations being within one order of magnitude from Guzek. However, the TALYS results did not show the slight increase in yield past 80 degrees for the 4.0 MeV incident protons, instead being monotonically decreasing for all examined energies. Additionally, the TALYS results did not show the magnitude to which the neutron response was forward peaked as identified by Guzek.
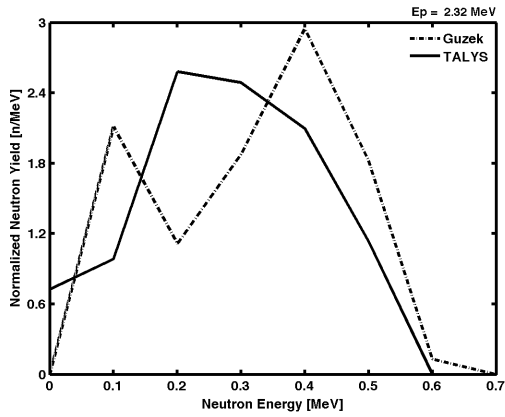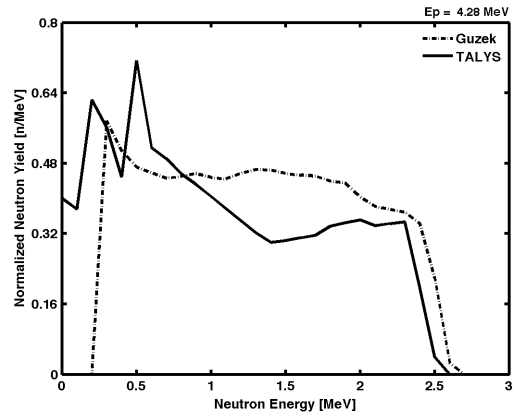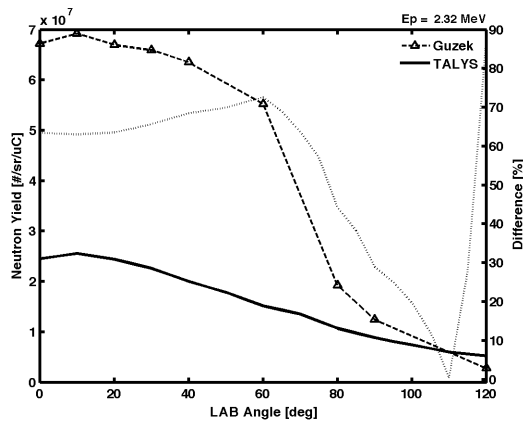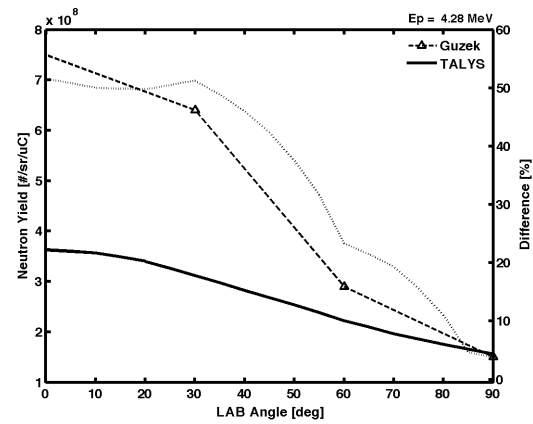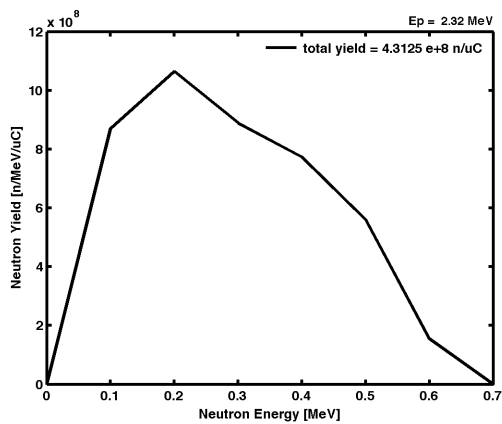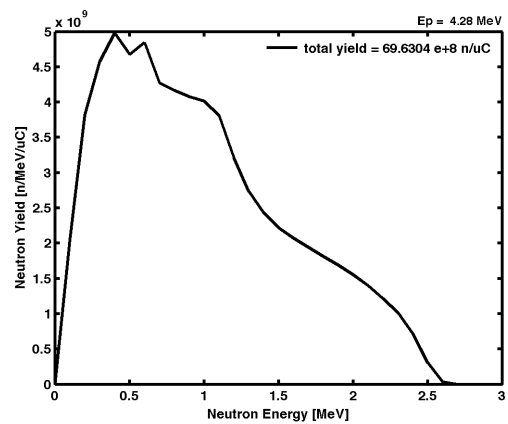
Figure 3-10: TALYS results for the ^{7}Li(p,n)^{7}Be reaction at 2.32 MeV ((a)-(c)) and 4.28 MeV ((d)-(f)), as compared to Guzek's results. Plots (a) and (d) show the normalized 0 degree calculation used in TALYS keyword optimization, plots (b) and (e) show the TALYS calculated angular yields and their difference with Guzek's results, and plots (c) and (f) show the TALYS calculated angle integrated total neutron yield curves.

44

3.6　Conclusions

All TALYS calculated results with incident deuterons displayed the gross characteristics of the the experimental data for each of the ion energy-ion-target combinations examined; however, certainly some results better approximated experiments. Results arising from incident protons were not as successful in characterizing the neutron response.

Calculations involving incident deuterons proved to be more adjustable than those involving incident protons with the inclusion of one keyword using the method described in Appendix A. It is possible that the proton results could be more finely tuned with combinations of two or more keywords, and this is a recommended area for exploration for users seeking to model a proton accelerator neutron source.

Additionally, the keywords identified only permitted limited adjustments to the neutron response curves. Inclusion of the selected keywords facilitated gross adjustments to the width of the low energy peaks, relative heights of the different neutron groups, location and slope of sharp increases/decreases, overall smoothness, and angular yields. The ability to modify the location of the peak energy in the response was notably absent using the the tuning methodology utilized in this thesis.

The discovery that keywords utilized in combination produced results not seen by individual modifiers was not surprising, as nuclear model calculations involve numerous coupled parameters. However, examining combinations of keywords using the method utilized in this thesis would be extremely computationally intensive; a more thoughtful and precise method of adjustment could possibly yield more suitable results.

The keyword optimization utilized the 0 degree spectrum because it was available across the data sets examined. Other methods of comparison may be appropriate for different intended uses of the source model, and it is important to note that the optimum keywords and keyword values are not necessarily the same for different goals. For example, matching of the 0 degree spectrum for the ^{7}Li(d,n)^{8}Be reaction yields different optimization results than matching with a focus on the angular yield curve.

Overall, the intended use of the source model and the acceptable tolerance of the spectrum will determine the appropriateness of the model. For instance, if the system parameters under consideration are the 0 degree response curve and the total neutron yield over 4π, the TALYS results for the ^{9}Be(d,n)^{10}B are generally accurate. If the same ion-target combination is under examination and the user is concerned about the yield at a specific output angle, the results are more suspect. For use in a particular application, it is recommended that the user attempt to optimize the calculations with two bounding incident energies, if available, in order to determine the limits of suitability.

With a neutron spectrum determined within an acceptable tolerance, other characteristics of the complete system can be explored in a virtual test bed. The spectrum then allows the user to identify and adjust system design parameters prior to construction of the system. This type of analysis is demonstrated in the following chapter with respect to neutron activation analysis.

Chapter 4

Activation Analysis

4.1 Activation Overview

The greatest neutron flux in an accelerator-based neutron source will be at the target, and it is therefore important to consider the activation of the materials holding the target when creating an experimental system model. The true importance and impact of this activation on the experimental setup will depend on the material's decay characteristics after activation and how that interferes with the desired signal. This thesis considers induced activity in general as undesirable, but makes a gross distinction in time as a means for illustrating various materials' decay characteristics.

Although data sheets are available that specify components of a certain material, they do not list all the impurities present. And because a relatively small amount of a substance in a mass can have a disproportionately large activity, it becomes necessary to investigate materials for highly active isotopes in order to characterize a material's activity. In this thesis, activation analysis is conducted by observing activity resulting from exposure to a reactor-based neutron source, and then extending those results to an accelerator-based neutron source whose characteristics are determined by the source model developed in Chapter 2.

The objective of this analysis is to demonstrate one potential application of the source model by approximating the relative activity expected of selected materials that may be subject to an intense neutron flux in an accelerator based system. This

analysis allows adding relative activity to material selection design parameters such as relative cost, thermal conductivity, etc. for the complete system.

The activation analysis was conducted on six test materials, listed in Table 4.1. With the exception of Zircaloy-4, these materials are common parts of accelerator construction and may be found in close proximity to the target, if not actually the target holder. For analysis, each sample was made small enough such that it would experience a near uniform flux while undergoing irradiation, and then reduced further for counting in order to achieve point source like geometry.

Table 4.1: Activation analysis test materials.

Abbreviation	Material
OFHC Cu	Oxygen-Free High Conductivity Copper
6061 Al	Aluminum Alloy Number 6061
SS 302	Stainless Steel Alloy Number 302
SS 316	Stainless Steel Alloy Number 316
Ti CP2	Commercial Pure Titanium Grade 2
ZR4	Zircaloy-4, a zirconium based alloy

The samples were irradiated in the MIT 5 MW Nuclear Research Reactor (MITR-II) in two fashions, differentiated by exposure time and neutron flux [10]. The short samples were irradiated for 10 seconds in a one inch pneumatic tube, designated 1PH, and experienced a thermal flux on the order of 10^{12} n/cm^2/s. The long samples were irradiated for two hours in a two inch pneumatic tube, designated 2PH, and experienced a thermal flux on the order of 10^{13} n/cm^2/s and a fast flux of up to 10^{12} n/cm^2/s. The flux characteristics of 1PH and 2PH are a result of their disposition within the reactor and graphite reflector, and the general time characteristics are determined by the experimental facilities.

After irradiation, the counting was conducted using a shielded Canberra germanium detector in conjunction with Genie 2000 software. The isotopes present in each sample were determined by examining the energies of the observed gamma lines, the relative ratios for isotopes with multiple lines, and the half-lives of the isotopes using both the Genie 2000 software and an online database [5]. The activity due to expo-

sure inside the reactor at the time the sample was removed, $A_{0,R}$, was calculated for each isotope by

$$A_{0,R} = \frac{(C-B)\lambda_i}{R(E)\epsilon_{det}(E)e^{\lambda_i t_0}\left(e^{-\lambda_i t_1} - e^{-\lambda_i t_2}\right)} \ , \qquad (4.1)$$

where C is the net area of an isotope's full energy peak recorded by the detector, B is the background counts, λ_i is the decay constant for isotope i, $R(E)$ is the decay branch ratio of the isotope at energy E, $\epsilon_{det}(E)$ is the efficiency of the detector at energy E, and t_0, t_1, and t_2 represent the time of irradiation, the time counting was started, and the time counting was completed [6]. The background counts were conducted separately for the short and long irradiations, and the efficiency of the detector as a function of energy was determined by the detector software after calibration.

4.2   Irradiation in MITR-II

The short samples were irradiated for 10 seconds and then allowed to decay for several minutes before being placed onto the detector. The samples were then counted for 10 minutes, allowed to decay for several more minutes, and then counted again for 30 minutes.

Table 4.2 displays the results of these counts. For each sample, the identifiable isotopes primarily responsible for the gamma ray counts are listed in the second column. The third and fourth columns indicate the ratio of the isotopes gamma peaks to the sum of the significant peak areas for a specified counting time. The final two columns indicate the activity per unit mass of the samples immediately after irradiation in the reactor, or $A_{0,R}$, and the associated relative uncertainty.[1]

The long samples were irradiated for 2 hours and then allowed to decay for several days before being placed onto the detector. The samples were then counted for 24 hours.

Table 4.3 displays the results of these counts. For each sample, the identifiable

---

[1]The relative uncertainty calculated for the short and long irradiation times considered only the statistical uncertainty associated with counting. That is to say the variables in Equation 4.1, with the exception of C and B were treated as having no uncertainty.

isotopes primarily responsible for the gamma ray counts are listed in the second column. The third column indicates the ratio of the isotopes gamma peaks to the sum of the significant peak areas for the entire counting time. The final two columns indicate the activity per unit mass of the samples immediately after irradiation and the associated relative uncertainty. The (n, γ) cross section data are not available for the As-71 isotope; however, treating its contribution as unknown does not appreciably impact results.

Table 4.2: Activation as a result of short irradiation.

Sample	Primary Gamma Contributors			Act., $A_{0,R}$	Rel. Uncert.
	[Isotope]	[% 10 m peaks]	[% 30 m peaks]	[μCi/g]	[%]
OFHC Cu	Cu-66	58.8	7.1	1.85 e+4	3.1
	Cu-64	41.2	92.9		
6061 Al	Al-28	88.1	72.6	2.25 e+4	1.8
	Mn-56	n/a	17.9		
	unknown	11.9	9.5		
SS 302	Mn-56	92.7	97.0	3.04 e+2	1.6
	unknown	7.3	3.0		
SS 316	Mn-56	91.2	95.2	3.39 e+2	1.1
	unknown	8.8	4.8		
Ti CP2	Ti-51	100.0	100.0	3.20 e+2	5.9
ZR4	Sn-125m	67.4	21.9	1.38 e+0	7.2
	Sn-123m	32.6	62.8		
	Zr-97	n/a	15.3		

4.3 Extension to Accelerator Sources

The initial activities based on the irradiation in the reactor, $A_{0,R}$, can be adjusted to reflect the anticipated activity based on exposure to the specific neutron flux associated with a particular ion-target combination. To illustrate this comparison, the adjustment resulting from 3 MeV deuterons incident on a thick beryllium target is presented. This correction was accomplished by first calculating the inner product of the reactor and accelerator's spectra production weights (after normalization) $wgt_i(E)$ with the radiative capture cross sections $\sigma_{n,\gamma}(E)$, or

$$P_i = wgt_i(E) \cdot \sigma_{n,\gamma}(E) \ . \tag{4.2}$$

For the short irradiations in the 1PH pneumatic tube, the entire neutron flux was assumed to be thermal, and so the thermal neutron cross section and a weight of 1 was used to determine P_R in that instance. For the long irradiations, P_R was determined using an MCNPX model of the reactor to generate $wgt_i(E)$ [11]. MCNPX version 2.6b was used to generate the 2PH reactor spectrum; this spectrum is shown in Figure 4-1 (a), and the model's geometry is shown in Figure 4-2. In all cases involving the accelerator spectra, P_T was determined using $wgt_i(E)$ generated by TALYS calculations. The TALYS generated accelerator spectrum is shown in Figure 4-1 (b). Finally, in all instances, $\sigma_{n,\gamma}(E)$ was obtained using JANIS software [1].

The activity was then corrected by multiplying the reactor initial activity after irradiation by the ratio of accelerator to reactor spectra, or

$$A_{0,T} = A_{0,R} \frac{P_T}{P_R} \tag{4.3}$$

The results of these adjustments are shown in Table 4.4, where $A_{0,R}$ represents the initial activity of the sample from the reactor, and $A_{0,T}$ represents the activity produced by the thick beryllium target. To facilitate a direct comparison, and as a result of normalization of the reactor-accelerator flux ratio, the activity listed for the accelerator-based source is what it would be if the accelerator had the same magnitude of flux as the reactor.

The relative uncertainties for $A_{0,R}$ were calculated as previously described, while the relative uncertainties for $A_{0,T}$ were calculated using assumed values of 0.35 percent for σ_{P_R}/P_R and 25 percent for σ_{P_T}/P_T. The value for σ_{P_R}/P_R was the highest uncertainty associated with the MCNPX simulation, and the value used for σ_{P_T}/P_T was the value for which the relative uncertainties for $A_{0,R}$ began to show significant change.
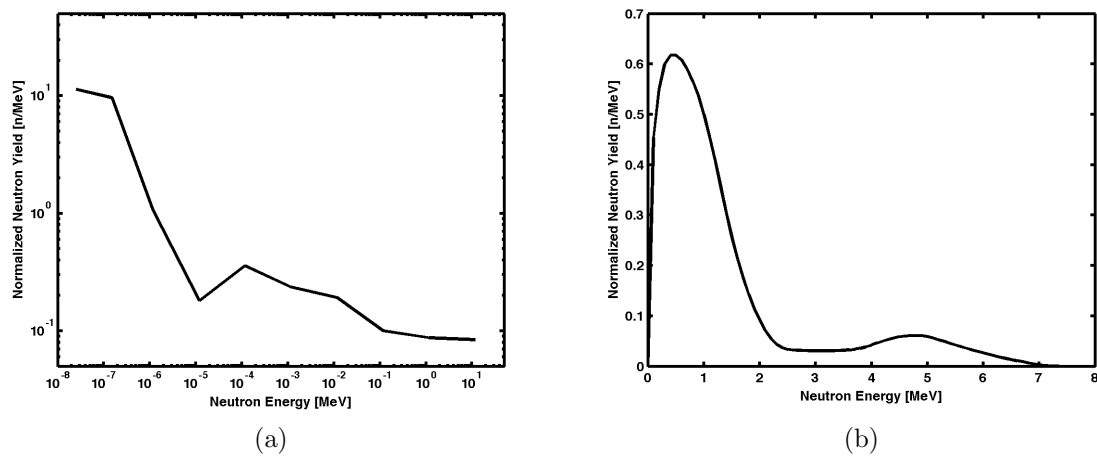
Figure 4-1: Normalized neutron spectra utilized in activation analysis. The MCNPX determined spectrum for the MITR-II 2PH pneumatic tube is shown in (a), and the TALYS determined spectrum over 4π for the ^{9}Be(d,n)^{10}B reaction at 3.0 MeV is shown in (b).
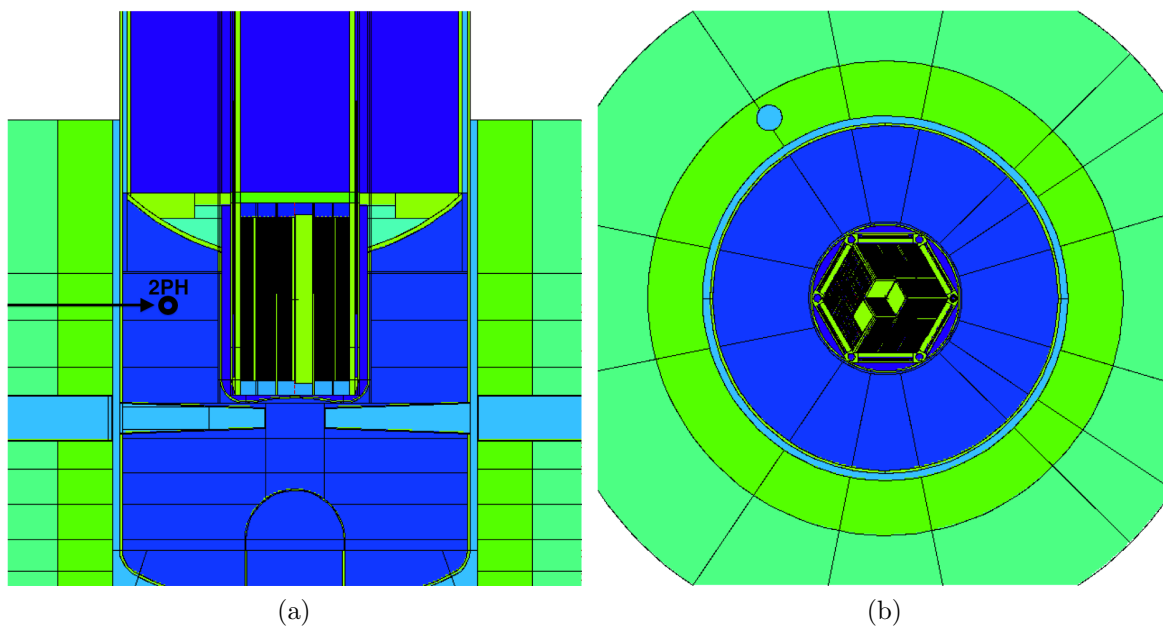
Figure 4-2: MITR-II MCNPX geometry, with side view (a) and top down view (b). The approximate location of the 2PH pneumatic tube is shown in (a)[11].

4.4 Conclusions

The time characteristics of the induced activation show that certain materials are more desirable for different applications. The optimum material would be determined by comparing the active isotopes' half-lives to the flux exposure time and desired signal counting window for the experiment. For example, if the flux exposure time and counting window is on the order of minutes, then aluminum would not be an ideal choice because the predominant short term isotope, Al-28, has a half-life of 2.24 minutes. However, in another application, the exposure time may be reduced or the counting window may be extended such that the 2.24 minute half-life is irrelevant. In a similar fashion, the long term activity may not be significant for any one period of time, but build up can occur if the exposure time is on the order of the long term half-lives and sufficient time is not allocated to allow those isotopes to decay away.

Another activation characteristic not discussed in this thesis is the decay energy of the activated isotope. Depending on the experimental setup, a certain decay energy may be discriminated against, thereby changing the relative importance of a material's isotopes. Considering either of the stainless steel alloys, the primary short time scale isotope is Mn-56 with approximately 80 percent of the observed activity resulting from the release of a 846 keV photon (the other 10 percent observed is due to a 1810 keV photon). Similarly, over half of the observed long time scale activity is the result of Cr-51 decay via a 320 keV photon. Thus, were an experimenter able to discriminate against a signal below 1 MeV, the majority of signal contamination due to induced activity would be eliminated.

This analysis is but one example of the possibilities that arise as the result of developing a working source model, beyond its most obvious deployment by characterizing the intended nuclear interactions of the system. As demonstrated, the source model is instrumental in creation of a virtual test bed, and facilitates designers' exploration of the system's operating characteristics and validation of key concepts prior to construction.

Table 4.3: Activation as a result of long irradiation.

Sample	Primary Gamma Contributors		Act., $A_{0,R}$	Rel. Uncert.
	[Isotope]	[% 24 h peaks]	[μCi/g]	[%]
OFHC Cu	Cu-64	63.6	1.63 e+6	5.8
	Ag-100m	22.4		
	Au-198	5.4		
	Sb-122	4.1		
	Sb-124	1.8		
	unknown	2.7		
6061 Al	Cr-51	89.5	1.12 e+1	0.3
	Zn-65	3.8		
	Fe-59	3.7		
	Sc-46	1.3		
	Co-60	1.1		
	unknown	0.6		
SS 302	Cr-51	88.6	3.33 e+3	0.2
	Fe-59	4.3		
	W-187	2.5		
	Co-60	1.5		
	Mo-99	1.2		
	unknown	1.9		
SS 316	Cr-51	60.3	4.03 e+3	0.1
	Mo-99	25.6		
	W-187	6.0		
	Fe-59	2.5		
	Co-60	2.3		
	unknown	3.3		
Ti CP2	Sc-47	77.5	4.44 e+1	0.7
	Sc-48	7.4		
	Sc-46	7.2		
	Cr-51	3.4		
	Sb-122	2.2		
	As-76	1.4		
	As-71	0.9		
ZR4	Zr-95	73.7	7.12 e+1	0.3
	Nb-95	13.8		
	Hf-181	4.8		
	Cr-51	4.0		
	Sn-113	0.6		
	Hf-175	0.3		
	unknown	2.8		

Table 4.4: Comparison between reactor and accelerator induced activities.

Sample	Short				Long			
	$A_{0,R}$		$A_{0,T}$		$A_{0,R}$		$A_{0,T}$	
	Act.	[Rel. Uncert.]	Act.	[Rel. Uncert.]	Act.	[Rel. Uncert.]	Act.	[Rel. Uncert.]
	[μCi/g]	[%]	[μCi/g]	[%]	[μCi/g]	[%]	[μCi/g]	[%]
OFHC Cu	1.85 e+4	3.1	6.97 e+1	3.2	1.63 e+6	5.8	6.86 e+3	6.0
6061 Al	2.25 e+4	1.8	4.75 e+3	1.8	1.12 e+1	0.3	8.93 e−1	0.3
SS 302	3.04 e+2	1.6	8.37 e−2	1.6	3.33 e+3	0.2	2.21 e+2	0.1
SS 316	3.39 e+2	1.1	9.34 e−2	1.1	4.03 e+3	0.1	2.89 e+2	0.1
Ti CP2	3.20 e+2	5.9	1.64 e+1	6.1	4.44 e+1	0.7	5.23 e−1	0.9
ZR4	1.38 e+0	7.2	1.61 e−1	6.9	7.12 e+1	0.3	2.28 e+1	0.4

Chapter 5

Conclusions and Future Work

Often, a neutron based application is conceived with specific characteristics of a neutron spectrum in mind. These characteristics may include total yield, the presence or absence of certain energy groups, angular behavior, etc., all of which are difficult to calculate and may not be present in the literature. The model presented in this thesis enables a user to determine a unique neutron spectrum based on five design parameters: incident ion energy, incident ion type, target material, target thickness, and outgoing neutron angle. Adjusting these parameters allows the user to broadly determine a combination necessary to produce the desired neutron spectrum.

The model created for this thesis was examined with respect to several ion-target combinations involving low atomic number, solid phase targets. These combinations do not have evaluated data libraries for direct use in Monte Carlo simulations, but enough published data were available to determine the efficacy of the model. The model produced useable results for the neutron response of ion-target combinations involving deuterons; however, it was less successful when characterizing the reactions produced by protons.

The model-produced neutron spectrum is well suited for use as a probability density function as part of a Monte Carlo based simulation such as MCNPX. This type of use enables the user to create a system model that includes the intended nuclear reactions of the system and continues through to a measured signal within the system's detectors. The model's results also facilitate other uses of the neutron spectrum, as

demonstrated with the activation analysis presented.

An important aspect of the model developed involves the tuning process using modifier keywords in the TALYS calculations. The tuning process implemented in this thesis enabled modification of the deuteron based results, but not for the proton based results. Future use of the model could include tuning with a more thoughtful selection of modifier keywords or incorporating the effects of multiple keywords into a iterative selection approach. It is recommended that use of the model is proceeded by first optimizing the inputs against available experimental data for bounding energies; this process will assist in determining the the limits of applicability. Finally, future use of the model could incorporate the effects on the neutron spectrum if the assumption of using an experimentally thick target is relaxed, and all the incident ions are not stopped within the target.

Appendix A

TALYS Keyword Test

This appendix describes the methodology used in this thesis to determine the keywords necessary to optimize the TALYS results to experimental data. Because this approach utilizes only one incident projectile energy, the keywords and the values examined will only provide a rough idea of which are necessary. Final adjustment of TALYS requires utilizing the full modeling process.

A text file was first created with the following columns: index, keyword, value 1, and value 2, as shown in table A.1. For the keywords with a numeric range, values were selected near the extremes in order to identify the impact their inclusion would have on the resultant spectrum. For keywords with binary entries, both were listed although one of them would be necessarily considered the default value. All keywords, with the exception of those requiring separate input files and those concerning output format, were explored.

Table A.1: Example keyword test file.

000.	aadjust	0.5	1.5
001.	adddiscrete	y	n
002.	addelastic	y	n
...	...	...	...

A UNIX script, shown starting on page 61, then ran TALYS over each combination of specified keyword and value, creating a folder for each combination. This script

utilized a keyword file with only two value columns; however it is possible to extend to an arbitrarily large number of columns to include more possible values with an adjustment in the script. Another way to get the same result without adjusting this script would be to add more rows to the keyword file with other possible values. The evaluation script should be run in the same directory as the keyword test file.

Finally, MATLAB was used to graphically inspect the results in order to determine which keywords affected the results and how. Each resultant spectrum was plotted on the same graph; thus, by viewing the plot in MATLAB's Plot Browser and highlighting the legend entries in sequence, one could determine the keywords needed to influence the spectrum's behavior. The MATLAB script used is shown on the following pages.

Of note in the MATLAB script is its reliance on the structure of the TALYS keyword test machine. It reads files created from the test machine as keyword indices and processes the data for both 0 degrees and integrated over all angles. The yield calculations and plots are in units of $\#/\mu$C for ease of comparison with experimental data. Finally, the script should be run in the same directory as the MATLAB script `importfile.m`, which is described in Appendix D.

```tcsh
#!/bin/tcsh
################################################################################
# reads a general set of parameters from the user
# iterates over a set of potential keywords, and:
#     - creates a directory for each keyword
#     - writes a talys input file with each keyword
#     - executes talys

echo -n "Input target element: "
 set element = $<
echo -n "Input target mass number: "
 set mass = $<
echo -n "Input projectile symbol: "
 set projectile = $<
echo -n "Input projectile energy: "
 set energy = $<

awk '{print $1" "$2" "$3}' 91.keyword\ base > 92.key-01
awk '{print $1" "$2" "$4}' 91.keyword\ base > 93.key-02

# the engine - loops over all keywords and values specified
set n = 1
while ($n < `wc -l 92.key-01 | awk '{print $1+1}'`)

# first  set of keyword values
set directory1 = `awk '(NR == "'"$n"'") \
                        {print 2*"'"$n"'"+99"."$2"_"$3}' 92.key-01`
mkdir $directory1
set keyword1 = `awk '(NR == "'"$n"'"){print $2" "$3}' 92.key-01`

echo \
"element $element\
mass $mass\
projectile $projectile\
energy $energy\
recoil y\
labddx y\
outangle y\
outspectra y\
ddxmode 2\
filespectrum n\
fileddxa n 0\
$keyword1"\
> input

mv input $directory1
cd $directory1
(talys115pgi < input > output) >> & error
cp ../importfile.m ./
if ( ! -e nddx000.0.lab ) rm *
echo "Done with $keyword1"
cd ..
```

```
# second set of keyword values
set directory2 = `awk '(NR == "'"$n"'") \
                        {print 2*"'"$n"'"+100"."$2"_"$3}' 93.key-02`
mkdir $directory2
set keyword2 = `awk '(NR == "'"$n"'"){print $2" "$3}' 93.key-02`

echo \
"element $element\
mass $mass\
projectile $projectile\
energy $energy\
recoil y\
labddx y\
outangle y\
outspectra y\
ddxmode 2\
filespectrum n\
fileddxa n 0\
$keyword2"\
> input

mv input $directory2
cd $directory2
(talys115pgi < input > output) >> & error
cp ../importfile.m ./
if ( ! -e nddx000.0.lab ) rm *
echo "Done with $keyword2"
cd ..

@ n++
end

(rmdir *) >> & error
ls | awk '$NF > 100 && $NF < 900' > 94.f_array
ls | awk '$NF > 100 && $NF < 900' | cut -c 1-3 > 95.f_index
ls | awk '$NF > 100 && $NF < 900' | awk '{print "n" $1}' | cut -c 1-4 > 96.n_array
ls | awk '$NF > 100 && $NF < 900' | awk '{print "a" $1}' | cut -c 1-4 > 97.a_array
################################################################################
```

UNIX Script for TALYS keyword test machine.

```
clear all
close all
clc

% gather needed constants
N = input('Enter target density (in #/cc): ');
R = input('Enter range of projectile in target (in cm): ');

% import needed indicies
f_array = importdata('94.f_array');
f_index = importdata('95.f_index');
n_array = importdata('96.n_array');
a_array = importdata('97.a_array');

% determine number of folders containing data
total = length(f_index);
ayield = zeros(total,1);
nyield = zeros(total,1);

figure(1)
for i=1:total
    cd (f_array{i})
    importfile('nddx000.0.lab');
    assignin('base',a_array{i},data)
    a = evalin('base',a_array{i});
    ayield(i) = sum(6.242e12*(1-exp(-N*R*1e-27*a(7:end,2))))*0.1;
    figure(1)
    hold on
    plot(a(:,1),6.242e12*(1-exp(-N*R*1e-27*a(:,2))))

    importfile('nspec004.000.lab');
    assignin('base',n_array{i},data)
    n = evalin('base',n_array{i});
    nyield(i) = sum(6.242e12*(1-exp(-N*R*1e-27*n(7:end,2))))*0.1;
    figure(2)
    hold on
    plot(n(:,1),6.242e12*(1-exp(-N*R*1e-27*n(:,2))))

    cd ..
end

figure(1)
legend(a_array)
legend('off')

figure(2)
legend(n_array)
legend('off')
```

MATLAB script for comparing keyword test results.

Appendix B

Multi-Energy TALYS Calculation

This appendix provides the UNIX shell script used to run TALYS with multiple input energies as determined by a TRIM calculation. This script should be run in a directory containing the TRIM output `IONIZ.txt` file, as well as the MATLAB scripts `importfile.m` and `importfile1.m`. The MATLAB scripts are discussed in Appendix D.

The script will examine the TRIM output file, determine reaction energies, and then run TALYS once for each energy. Each energy will have it's own folder containing the TALYS input and output files, as well as copies of the MATLAB scripts needed to process the data.

Of note, the portion of the script describing the creation of the TALYS input file is provided not as used, but in an illustrative manner. In order to use the script, the user must remove the comments contained in the `echo` statement and all ellipsis. It is also necessary to use the TALYS executable specific to the user's computer.

Finally, the portion of the script used in determining the particle production weights for neutrons and photons using the non-elastic cross sections is included for completeness. Ultimately, the total cross sections were used in the thesis, but the non-elastic methodology and reasons for not using it are described in Appendix C.

```tcsh
#!/bin/tcsh
################################################################################
# part 1 - gather needed information from SRIM/TRIM, determine energies
# read output file from SRIM/TRIM calculation
# integrate -dE/dx to get reaction energy for each depth bin
# select every 3rd energy to comprise input energies for TALYS
# read IONIZ.txt output file from SRIM/TRIM calculation

echo "depth [cm]      eloss [MeV/cm]" > bragg
tail -100 IONIZ.txt | \
awk '{depth = $1 * 1E-8} \
     {loss = $2 * 1E2} \
     {printf "%-15.4E %-15.4E\n", depth, loss}' >> bragg

# determine width of depth bins
set delta = `head -2 bragg | grep -v depth | awk '{print $1}'`

# integreate -dE/dx to determine energy lost getting to a particular bin
echo "depth [cm]      eloss [MeV/cm]  elost [MeV]" > integrated
awk '{lost += $2 * "'"$delta"'"} \
     {if ($2 > 0) printf "%-15.4E %-15.4E %-15.4E\n", $1, $2, lost}' \
     bragg >> integrated

# read incident deuteron energy from IONIZ.txt file
set incident = `awk '/keV/ {print $6/1000}' IONIZ.txt`

# determine reaction energy for each depth bin
echo "depth [cm]      rxn e [MeV]" > reaction
awk '{rxne = "'"$incident"'" - $3} \
     {if ($1 > 0) printf "%-15.4E %-15.4E\n", $1, rxne}' \
     integrated >> reaction

# select specified interval of energies for reaction
# picks every 3rd energy bin
awk '((NR % 3) == 0) {printf "%-7.4f \n", $2}' reaction | sort -g > energies

echo "Energies selected."

# set energy variable equal to range of energies
set energy = `cat energies`

# bookkeeping --> make directories and initialize cross section files
mkdir gamma neutron
echo "energy gprod xs" > gamma/gprod
echo "energy nprod xs" > neutron/nprod
echo "energy non-e xs" > nonelastic

################################################################################
# part 2 - the calculation engine
# for each energy selected:
#     - create TALYS input file
#     - run TALYS
```

```
#      - copy spectra files to single folder
#      - copy non-elastic and production cross sections to a single file

# begin loop over each distinct energy value
foreach energy ($energy)

# create a separate energy directory and change into that directory
mkdir $energy
cd $energy

# create input file for TALYS
echo \
"element be\       # four mandatory keywords for TALYS calculations
mass 9\           #
projectile d\     #
energy $energy\   #

recoil y\         # keywords necessary for spectra files
labddx y\         #
outangle y\       #
outspectra y\     #
ddxmode 2\        #
filespectrum n g\ #

fileddxa n 0\     # list all angles of interest
fileddxa n 5\     #
fileddxa n 10\    #
 ...              #

maxlevelsbin n 5\ # list all modifier keywords
  ...
  ..."\
> input

# run TALYS v1.15 w/ pgi compiler on input file
talys115pgi < input > output

# copy particle spectra files to specified folder
(cp gspec*.lab ../gamma ) >> & error
(cp nspec*.lab ../neutron) >> & error

# amend files containing particle production and non-elastic cross sections
awk '/gamma / && /Multiplicity=/ {print "'"$energy"'", $3}' \
    output >> ../gamma/gprod
awk '/neutron / && /Multiplicity=/ {print "'"$energy"'", $3, $5}' \
    output >> ../neutron/nprod
awk '/Non-elastic    = / {print "'"$energy"'", $3}' \
    output >> ../nonelastic

# bookkeeping--> copy MATLAB file to directory, clear non-relevant directories
cp ../importfile.m importfile.m
if ( ! -e nddx000.0.lab ) rm *

# print confirmation to terminal, change back to parent directory
```

```
echo "Done with" $energy "MeV calculation."
cd ..

# end loop, remove non-relevant directories, print confrimation to terminal
end
(rmdir *) >> & error
echo "TALYS calculations complete."


################################################################################
# part 3 - determining production weights based on non-elastic cross sections
# determine probability of producing particles in each depth bin
# read atom density from IONIZ.txt file, determine width of reaction bins

set density = `awk '/cm3/ {print $6}' IONIZ.txt`
set delta = `awk '((NR % 3) == 0)' reaction | \
     sort -g | \
     awk '{new=$1} \
          {if (NR==1) low = $1} \
          {if (NR==2) high = $1} \
          {print (high-low)}' | \
     awk 'NR==2'`

# determine the probability of not reacting in each depth bin
sort -r nonelastic | \
     awk '{if (NR>1) printf "%-7.4f %-10.7E \n", $1,  \
          exp(-($2*1E-27) * "'"$density"'" * "'"$delta"'")}' \
     > norxndx

# determine the probability of the incident particle reaching each depth bin
awk 'BEGIN {norx = 1}; \
     {printf "%-7.4f %-10.7E \n", $1, norx=norx*$2}' \
     norxndx > norxn

# determine the probability of reacting in each depth bin
awk '{printf "%-7.4f %-10.7E \n", $1, 1-$2}' norxndx > rxndx

# determine the probability of reaching each depth bin, and then reacting
paste norxn rxndx | awk '{printf "%-7.4f %-10.7E \n", $1, $2*$4}' > rprob

# sort cross section files, and change units to cm^2
sort -r neutron/nprod | awk '{if (NR>1) \
                               printf "%-7.4f %-10.7E \n", $1, $2 * 1E-27}' > nxs
sort -r gamma/gprod | awk '{if (NR>1) \
                             printf "%-7.4f %-10.7E \n", $1, $2 * 1E-27}' > gxs
sort -r nonelastic | awk '{if (NR>1) \
                            printf "%-10.4f %-10.7E \n", $1, $2 * 1E-27}' > none

# merge cross section files into one table
paste none rprob nxs gxs | \
     awk '{if ($2>0) printf "%-10.4f %-10.7E %-10.7E %-10.7E %-10.7E \n", \
          $1,$2,$4,$6,$8}' > table

# determine the probability of reaching each depth bin,
#     and then producing a particle
```

```
awk '{nwt = $3 * $4 / $2} {printf "%-7.4f %-10.7E \n", $1, nwt}' \
    table | sort > neutron/nweight
awk '{gwt = $3 * $5 / $2} {printf "%-7.4f %-10.7E \n", $1, gwt}' \
    table | sort > gamma/gweight

# bookkeeping --> write arrays, copy MATLAB files,
#     move files to holding directory
awk '{printf "%-10.7E \n", $2}' neutron/nweight > neutron/nweights
awk '{printf "%-10.7E \n", $2}' gamma/gweight > gamma/gweights
cp neutron/nweights nweights
cp importfile.m neutron/importfile.m
cp importfile.m gamma/importfile.m
mkdir results working
mv importfile1.m working/
mv bragg working/
mv energies working/
mv error working/
mv gxs working/
mv integrated working/
mv IONIZ.txt working/
mv none working/
mv nonelastic working/
mv norxn working/
mv norxndx working/
mv nxs working/
mv reaction working/
mv rprob working/
mv rxndx working/
mv table working/

# print confirmation to terminal
echo "Weight calculations complete."
################################################################################
```

UNIX Script for multi-energy TALYS calculation.

Appendix C

Non-Elastic Calculation

This appendix describes the methodology used to calculate the probability of an incident particle reaching a particular depth bin, and then undergoing a non-elastic collision in which the particle of interest is produced. This calculation considers incident particles experiencing an elastic collision within the target as still being available for a non-elastic collision, albeit without a reduced energy, and comprises the last portion of the script in Appendix B. However, because the difference between this method and calculations involving the total cross sections was essentially zero, the simpler method of using the total cross section was used in this thesis.[1] The method is illustrated below using 3 MeV deuterons incident on a thick beryllium target.

The TALYS output files and calculated cross sections were read and analyzed to produce weighted spectra for outgoing neutrons and photons using a UNIX shell script. First, the probability of not reacting in each depth bin, $p_{norxndx}$, was calculated by

$$p_{norxndx} = e^{-\sigma_{non-el}(E)N\Delta x} \ ,$$
(C.1)

where $\sigma_{ne}(E)$ is the deuteron's non-elastic microscopic cross section at energy E, N

---

[1]The difference was determined by the ratio of the difference between the two values to one of the values, as was calculated in Equation 3.1. The simplicity gained by considering the total cross sections was realized in the post-TALYS calculation processing in a MATLAB script. Using the non-elastic particle production method required additional normalization, especially when computing the angular spectra.

is the atom density of the beryllium target, and Δx is the width of each depth bin.

This value was then used to calculate the probability of the deuteron getting to each successive depth bin without undergoing a non-elastic collision, p_{norxn}, and the probability of reacting in each particular depth bin, p_{rxndx}. p_{norxn} was determined by calculating the product of not reacting in each depth bin leading up to the bin of interest, or

$$p_{norxn} = \prod_{i=1}^{N-1} p_{norxndx,i} \; , \tag{C.2}$$

where i is an index representing each depth bin and N is the bin of interest. p_{rxndx} was determined by subtracting $p_{norxndx}$ from unity.

Finally, the probability of undergoing a non-elastic scattering event for each depth bin, p_{rxn}, was determined by multiplying the probability of getting to that bin without undergoing a non-elastic reaction and the probability of reacting inside that particular bin, or

$$p_{rxn} = p_{norxn} \cdot p_{rxndx} \; . \tag{C.3}$$

The reaction weights for each incident energy $wgt(E)$ was determined by calculating the probability of undergoing a non-elastic collision in a particular depth bin (corresponding to a certain reaction energy), and then multiplying that by the ratio of particle production cross section to non-elastic cross section, or

$$wgt(E) = \frac{\sigma_{prod}(E)}{\sigma_{non-el}(E)} \cdot p_{rxn} \tag{C.4}$$

These weights therefore described the probability of producing a neutron per incident deuteron at a certain energy. A comparison between this method and the total cross section is presented in Figure C-1.

The similarity between the methods' results is expected considering the small total cross section for the ion-target combinations considered. This small total cross section translates to a mean free path on the order of tens of centimeters, which, when considering an experimentally thick target on the order of at most a few hundred microns, means that the probability of interaction is very small.
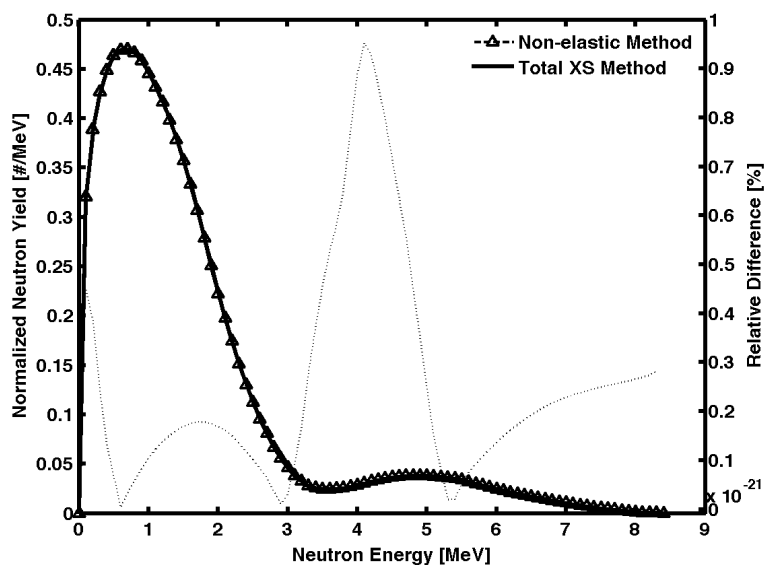
Figure C-1: Non-elastic cross section vs. total cross section comparison methodology. This plot shows the normalized angle integrated neutron yield for a 3 MeV deuteron beam incident on a thick beryllium target. The triangles represent results using non-elastic cross section methodology, and the solid line represents the total cross section methodology. The fine dashed line shows the relative difference between the two approaches.

Although not utilized in calculating the results presented in this thesis, the method of calculation described in this appendix was useful as a secondary confirmation of the results presented.

Appendix D

TALYS Processing with MATLAB

This appendix provides the MATLAB script used to process TALYS output files. The script should be run from the reaction's parent directory containing all the incident energy folders generated from the UNIX script and TALYS calculations.

Of note is the user interface that requires entering parameters needed to perform calculations, plot results, and create specific file names. If the user is performing multiple instances for the same setup, it may be less tedious to specify these values; they are written here to illustrate the need to adjust them based on the system modeled.

Not included are two subscripts called during its execution, `importfile` and `importfile1`, which are MATLAB generated scripts that read text files into data arrays. The `importfile` script is utilized to read the TALYS output files and accounts for the files having five header lines. The `importfile1` script performs the same function, but on the UNIX script generated files, for which there is only one header line.

```
%% clear workspace, gather input ---------------------------------- %%
clear all
close all
clc

% variable definitions
% bwidth = specified depth bin interval from TRIM output
% awidth = specified angle interval from TALYS input file [deg]
% findex = file index for saving results/plots
% energy = incident particle energy [MeV]
% target = symbol for target
% incpar = symbol for incident particle
% tarden = target density [atoms/cc]
% c_date = current date [yyyy-mm-dd]
% deltax = bin width distance [cm]
% egybin = number of energy bins
% egyrxn = array of reaction energies
% nspecr = raw differential cross sections from TALYS output
% maxegy = maximum energy from neutron output spectrum [MeV]
% ntrin1 = index of neutron output energies [MeV]
% sindex = size of neutron output energy index
% ntregy = neutron output energy matrix, each input energy has a column
% nspect = total neutron spectrum
% nspeci = neutron output energy matrix, interpolated to common index
% ntryd1 = neutron yield calculated by .nspec files
% angbin = number of angle bins
% ntrang = raw double differential cross sections from TALYS output
% ntrin2 = index of neutron output energies [MeV]
% tangle = output angle spectra matrix
% totala = total spectrum integated over output angles
% ntrddx = neutron output matrix, interpolated to common index
% aindex = index of angles
% ntryd2 = neutron yield calculated by .ddx files
% angyd0 = angular yield for 0 degrees
% ylddif = yield difference

% gather input for inclusion into calculations, plots, and filenames
bwidth = input('Enter depth bin interval (1=every bin): ');
awidth = input('Enter anglular interval [deg]: ');
findex = input('Enter file index: ', 's');
energy = input('Enter incident particle energy [MeV]: ','s');
target = input('Enter target material: ', 's');
incpar = input('Enter incident particle: ', 's');
tarden = input('Enter target atomic density [atoms/cc]: ');
c_date = datestr(now, 29);

cd working
importfile1('reaction');
d0 = data;
deltax = d0(bwidth+1);
clear d0
cd ..
```

```matlab
d1=[];
for i=1:str2double(energy)+1
    d1 = [d1; dir([num2str(i-1) '.*'])];
    d2 = {d1([d1.isdir]).name}.';
end

egybin = numel(d2);

for i=1:egybin
    egyrxn(i) = str2num(d2{i});
end

%%  energy spectra / energy spectra / energy spectra / energy spectra  %%
%% process neutron data ---------------------------------------------- %%
% change into neutron directory, identify spectrum files
cd neutron
d3 = dir('*.lab');
d4 = {d3.name};

% loop over each energy, place spectra into multi-dimensional array
for e = 1:egybin
    cfile = d4{e};
    importfile(cfile);
    nspecr{e} = data;
    clear data;
end

% identify maximum energy of spectrum
maxegy = ceil(max(nspecr{egybin}(:,1))*10)/10;

% create common energy index
ntrin1 = [0:0.1:maxegy]';

% record size of index
sindex = size(ntrin1,1);

% pre-allocate vectors and prepare to merge
%      ntregy = spectrum matrix, each input energy has a column
%      nspect = total spectrum, sum of all contributions
ntregy = zeros(sindex,egybin);
nspect = zeros(sindex,1);

% loop over each energy, and:
%      match spectrum to common energy index by interpolation
%      remove parts that are non numbers
%      normalize to neutrons produced, weight by production probability
%      integrate over all energies
for e = 1:egybin
    nspeci{e} = interp1(nspecr{e}(:,1),nspecr{e}(:,2),ntrin1);
    nspeci{e}(isnan(nspeci{e})) = 0;
    ntregy(:,e) = 6.242e12*(1-exp(-tarden*deltax*1e-27*(nspeci{e})));
    nspect = nspect + ntregy(:,e);
end
```

```matlab
% change back to parent directory
cd ..

% calculate flux --> n produced per uA
nspect = [ntrin1,nspect];
ntryd1 = sum(nspect(:,2)) * 0.1;

%%          angular spectra / angular spectra / angular spectra      %%
%% gather data and pre-process data ------------------------------- %%
% loop over each energy, identify all angular spectrum files
for i = 1:egybin
    cd (d2{i})
    d5 = dir('*.0.lab');
    d6 = {d5.name}.';
    angbin = numel(d6);

    % loop over each angle, place spectra into muli-dimensional array
    for j = 1:angbin
        cfile = d6{j};
        importfile(cfile);
        ntrang{i,j} = data;
        clear data;
    end

% change back to parent directory
    cd ('..')
end

% identify maximum energy of spectrum
maxegy = ceil(max(ntrang{egybin,1}(:,1))*10)/10;

% create common energy index
ntrin2 = [0:0.1:maxegy]';

% record size of index
sindex = size(ntrin2,1);
% pre-allocate vectors and prepare to merge
tangle = zeros(sindex,angbin);     % output angle spectra matrix
totala = zeros(angbin,1);      % total integrated over output angles

for j = 1:angbin
    for i = 1:egybin
        ntrddx{i,j} = interp1(ntrang{i,j}(:,1),ntrang{i,j}(:,2),ntrin2);
        ntrddx{i,j}(isnan(ntrddx{i,j})) = 0;
        ntrddx{i,j} = 6.242e12*(1-exp(-tarden*deltax*1e-27*ntrddx{i,j}));
        tangle(:,j) = tangle(:,j) + ntrddx{i,j};
    end
    totala(j) = sum(tangle(:,j))*0.1;
end

% %% save data ------------------------------------------------- %%
% save results of neutron spectrum
file = ['findex '. ' energy ' MeV (' incpar ',' target ') nspec (' ...
```

```
    c_date ').txt'];
save(file,'nspect','-ascii')

% create indexed matrix and save angular data
aindex = [0 : awidth : 180];
tangle = [aindex; tangle];
tangle = [[0;ntrin2], tangle];
file = ['findex '. ' energy ' MeV (' incpar ',' target ') aspec (' ...
    c_date ').txt'];
save(file,'tangle','-ascii')
```

MATLAB script for processing TALYS output files.

Bibliography

[1] OECD Nuclear Energy Agency. "Java-based Nuclear Data Display Program (JANIS 3.1)." [Online] Available: http://www.nea.fr/janis/. [Accessed: April 1, 2010].

[2] F.M. Baumann, B. Bruggermann, H. Freiesleben, Th. Grodotzki, and H. Chr. Hilber. Energy Distribution and Yield of Neutrons from the (p,n) Reaction in Thick LiF Targets. *Nuclear Instruments and Methods*, A238:443–452, 1985.

[3] F.M. Baumann, G. Domogala, H. Freiesleben, H.J. Paul, S. Puhlvers, and H. Sohlbah. The 9Be(d,n)10B Reaction as Intense Neutron Source with Continuous Energy Spectrum. *Nuclear Instruments and Methods*, A247:359–366, 1886.

[4] Jacek Guzek. *Elemental Radiography Using Fast Neutron Beams*. PhD dissertation, University of the Witwatersrand, South Africa, March 1999.

[5] Korea Atomic Energy Research Insitute. "Table of Gamma Rays." [Online] Available: http://atom.kaeri.re.kr/gamrays.html. [Accessed: April 1, 2010].

[6] Glenn F. Knoll. *Radiation Detection and Measurement.* John Wiley & Sons, New York, 2000.

[7] A.J. Koning, S. Hilaire, and M.C. Duijvestijn. "TALYS-1.0", *Proceedings of the International Conference on Nuclear Data for Science and Technology - ND 2007*, May 22-27, 2007, Nice, France, editors O. Bersillon, F. Gunsing, E. Bauge, R. Jacqmin, and S. Leray, EDP Sciences, 2008, pages 211-214.

[8] A.J. Koning, S. Hilaire, and M.C. Duijvestijn. "TALYS-1.2." [Online] Available: http://www.talys.eu/. [Accessed: April 1, 2010].

[9] Mark Mitchell. "Engauge Digitizer - Digitizing Software." [Online] Available: http://digitizer.sourceforge.net/. [Accessed: April 1, 2010].

[10] Massachusetts Institute of Technology. "The MIT Nuclear Reactor Laboratory." [Online] Available: http://web.mit.edu/nrl/www/index.html. [Accessed: April 1, 2010].

[11] Everett Redmond. "MITR-II Full Reactor Model with ICSA and 3GV5". Made available by Tom Newton, MITR-II Reactor Operations, 1989.

[12] S. Whittlestone. Neutron Energy Spectra from the Thick Target 9Be(d,n)10B Reaction. Technical report, Australian Atomic Energy Commission, December 1976.

[13] S. Whittlestone. Neutron Distributions from the Deuteron Bombardment of a Thick Beryllium Target. *Journal of Physics D: Applied Physics*, 10:1715–1723, 1977.

[14] J.F. Ziegler. "The Stopping and Range of Ions in Matter." [Online] Available: http://www.srim.org/. [Acessed: April 1, 2010].

[15] J.F. Ziegler, J.P. Biersack, and U. Littmark. *The Stopping and Range of Ions in Solids.* Pergamon Press, New York, 1985.